QATAR UNIVERSITY

COLLEGE OF PHARMACY

ANTICANCER EFFECTS OF MODIFIED CITRUS PECTIN AND CURCUMIN IN CHITOSAN NANOPARTICLES ON COLON CANCER

BY

AREEJ A. AL HAMS

A Thesis Submitted to

the College of Pharmacy

in Partial Fulfillment of the Requirements for the Degree of

Masters of Science in Pharmacy

June 2022

COMMITTEE PAGE

The members of the Committee approve the Thesis of
Areej Al Hams defended on 28/04/2022.

Nashiru Billa
Thesis/Dissertation Supervisor

Hesham Korashy
Committee Member

Shahab Uddin Khan
Committee Member

Approved:

Mohammad Diab, Dean, College of Pharmacy

ABSTRACT

AL HAMS, AREEJ, A., Masters : June : [2022], [Pharmaceutical Sciences]

Title: Anticancer Effects of Modified Citrus Pectin and Curcumin in Chitosan Nanoparticles on Colon Cancer.

Supervisor of Thesis: Nashiru, Billa.

We aimed to study the influence of stirring effect while modifying citrus pectin (CP), in addition to create a combination of curcumin in chitosan-modified citrus pectin (CCM-NPs) nanoparticles, along with Galectin-3 in MCP, to produce more effective and possibly free from side effects chemotherapeutics and to improve the galectin yield to enhance the anticancer properties further and improve the specificity as well. CP was modified and the curcumin in chitosan-MCP nanoparticles (CCM-NPs) were formed by ionic gelation. The MCP formulations were studied as a function of stirring duration and the samples were labeled as MCP1, MCP2, and MCP4. The optimum conditions of adding STTP, CS, CUR, and the three formulations prepared (MCP1, MCP2, and MCP4) were studied to prepare the nanoparticles. The MCP1 formulation resulted the smallest size and the best zeta-potential values in comparison to MCP2 and MCP4 when STPP and CS concentrations were varied (STPP-MCP1-NPs showed a size of 240.6 $\pm$ 0.60 nm and a zeta-potential of 5.83 $\pm$ 0.01 mV when STPP concentration was varied, CS-MCP1-NPs showed a size of 173.6 $\pm$ 0.35 nm and a zeta-potential of 4.56 $\pm$ 0.01 mV when CS concentration was varied). When the amounts of STPP and CS were varied, 1AC showed as size of 209.4 $\pm$ 0.36 nm and a zeta-potential of 10.6 $\pm$ 0.02 mV when the amounts of STPP were varied, and 2AC showed a size of 139.3 $\pm$ 0.57 nm and a zeta-potential of 16.6 $\pm$ 0.02 mV when the amounts of CS were varied. Lastly, when CUR amounts were varied, 3CC showed a size of 351.1 $\pm$ 0.53 nm and a zeta-potential of 9.74 $\pm$ 0.03 mV.

The diffractogram of curcumin shows multiple peaks between 5° and 30° which were mainly attributed to its crystalline nature. These distinctive peaks were disappeared in the CCM-NPs, implying that curcumin's crystalline constitution had given way to an amorphous state. The morphology of the MCP-NPs and CCM-NPs were investigated using SEM and AFM, and the images indicated an evenly dispersed and spherically shaped nanoparticles. The thermogravimetric analysis of raw materials and CCM-NPs were studied, and the encapsulation efficiency was found to be 99.63%. A curcumin stability test as a function of light was applied and resulted that curcumin degrades the fastest when it is exposed to direct sun light. The curcumin stability in the prepared nanoparticles (CCM-NPs) was studied in different storages (at 4°C and 37°C) and resulted that the nanoparticles are more stable in cold temperatures in comparison to warm temperature. These findings point to the potential application of the encapsulation of curcumin in chitosan-MCP nanoparticles in the delivery of curcumin in the treatment of colon cancer. In vitro cell studies showed that CCM-NPS reduced the viability of colorectal cancer cell lines (HCT-116) by 54.74% $\pm$ 0.01% in comparison to free curcumin which reduced 18.69% $\pm$ 0.51% of cancer cells at a period of 48 hours. In conclusion, our findings demonstrated that this drug delivery system is a highly promising therapeutic approach, potentially leading to a future therapy option for colorectal cancer.

DEDICATION

Dedicated to my beloved family, for always believing in me, and to what I can accomplish surrounded with their endless love, continuous support, and sacrifices.

ACKNOWLEDGMENTS

I would like to thank Almighty Allah who gave me patience, strength, determination, resoluteness, and ceaseless blessings and mercy to keep going and pushing forward to accomplish my research. I would like to sincerely thank my supervisor Prof. Nashiru Billa, for his assistance, guidance, support, and patience that shaped the success of this research. I would also like to thank my co-supervisor, Prof. Hesham Korashy for his support throughout my cell work part. The time and effort, both professors placed into my project are deeply appreciated.

I would like to thank the technical staff in the college of Pharmacy, and more specifically, Ms. Aida Ghafar and Ms. Jensa Joseph for their continuous helpful and support on my experimental problems. I really appreciate their time, effort, and never hesitating to provide me with the help I need to succeed my research. I am also appreciative to Dr. Takwa Bedhiaifi from HMC for sharing her precious experience and trainings. My profound and sincere gratitude goes to my friend and college Ms. Sourour Idoidi, for her sharing this journey with me, and for her continuous support that ease my research journey. You made my days during the research journey remarkable. I am very grateful for the friends I made here, and more specifically Ms. Arij Hassan. You were a sounding board for anything I needed.

I will forever be grateful to all my family members, especially my parents. It would not happen without their unconditional love, mental and spiritual support which provides me with confidence to pursue my biggest dreams. Finally, I would like to thank the college of Pharmacy of Qatar University, the department of pharmaceutical sciences, for providing all the needed tools and equipment that are needed for this project. My appreciation and gratefulness go to Dr. Fatima Mraiche for her sincere support and for always reminding me of my biggest goals.

TABLE OF CONTENTS

LIST OF TABLES

LIST OF FIGURES

ABBREVIATIONS

ACN	Acetonitrile
AFM	Atomic Force Microscopy
ANOVA	Analysis of variance
CCM-NPs	Curcumin in Chitosan-Modified Citrus Pectin Nanoparticles
CP	Citrus pectin
CRC	Colorectal Cancer
CS	Chitosan
DMEM	Dulbecco's Modified Eagle Medium
DMSO	Dimethyl Sulfoxide
DLS	Dynamic Light Scattering
EE	Encapsulation efficiency
FBS	Fetal bovine serum
FT-IR	Fourier Transformed Infrared Spectroscopy
Gal-3	Galectin-3
GIT	Gastrointestinal tract
GS	Substituted galacturonans
hr	Hour
hrs	Hours
HG	Homogalacturonan
HPLC	High Performance Liquid Chromatography
IC_{50}	Growth inhibitory concentration
KBr	Potassium bromide
MCP	Modified citrus pectin

MCP1	Modified citrus pectin stirred for 1 hour
MCP2	Modified citrus pectin stirred for 2 hours
MCP4	Modified citrus pectin stirred for 4 hours
MCP-NPs	Modified citrus pectin nanoparticles
MeOH	Methanol
min	Minute
NaOH	Sodium hydroxide
NPs	Nanoparticles
PBS	Phosphate-buffered saline
pDI	Polydispersity index
RG-I	Rhamnogalacturonan-I
RG-II	Rhamnogalacturonan-II
SEM	Scanning Electron Microscope
STPP	Sodium tripolyphosphate
TGA	Thermogravimetric analysis
UV	Ultraviolet
WHO	World Health Organization
XRD	X-ray Powder Diffractometry
MeOH	Methanol
NPs	Nanoparticles

CHAPTER 1: INTRODUCTION

1.1 General overview

Cancer is a major public health problem worldwide, especially in the developed countries such as United States of America (USA) and Europe. Apart from the localized anatomical damage of the site of manifestation of cancer, it can spread almost anywhere in the human body through trillions of cells that replicate rapidly (1). According to Hamad Medical Corporation (HMC), colon cancer is the third most common manifestation of cancer in Qatar and this statistic has led to cancer-related deaths in both genders in the country (2). Recent statistics indicate that this trend will get worse. The most common treatment option in colon cancer is chemotherapy, which is apt with punishing side effects. Therefore, there is the need for the utilizing anticancer agents that present lesser side effects. Thus, there is a move towards finding effective anticancer treatments that manifests lesser side effects. In this regard, studies have shown that metastatic cells in many cancer types, such as colon and prostate cancers, can be suppressed by modified citrus pectin (MCP) (3). Pectin is a soluble fiber that is naturally present in the plants and in citrus fruit pulp and peel (4). It has been found that the galectin moiety in Modified Citrus Pectin (MCP), is specifically antagonistic to the metastatic and tumor cascade during the development of colon cancer (5,6). Thus, one of the key motivations to the present project concerns the methods for modification of citrus pectin whereby we believe that yield of galectin moieties after modification can be improved. We aim to improve the galectin yield during modification of pectin in an attempt to enhance the anticancer properties of MCP and further improve its specificity as well on colon cancer.

A further motivation to the present work is in addressing the issue of severe side effects associated with the use of chemotherapeutic drugs. In this regard, curcumin, a

polyphenol has been studied extensively for its anti-colon cancer effect. It manifests lesser toxicity to cells, however, it suffers from poor solubility, rapid clearance and low bioavailability and stability (7,8) (Figure 1.1). Through appropriate encapsulation, it is possible to improve uptake of curcumin. For example, curcumin has been formulated in chitosan nanoparticles in an attempt to surmount the biological barriers to absorption (8). We believe a combination of curcumin in chitosan nanoparticles along with MCP forms a potent therapeutic option in the quest for specific anti-colon cancer effect (9-11).

In patients with colon cancer, chemotherapeutic agents present several side effects, and it is necessary to concentrate on agents that manifest less effects and specific to colon cancer. Through the combination of curcumin in chitosan-MCP nanoparticles, along with improved galectin yield in MCP (which is involved in many biological behaviors such as apoptosis) (12). Thus, the anti-colon cancer intervention is deemed to be more effective and possibly free from side effects observed when using chemotherapeutics.

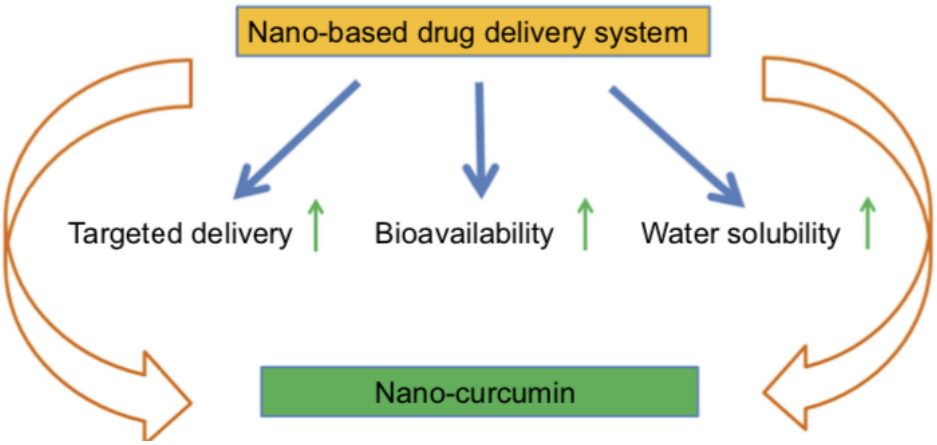

Figure 1.1 Nano-based drug delivery of curcumin-loaded nanoparticles to enhance the bioavailability and water solubility of curcumin. Adapted from (7).

1.2 Colon and colorectal cancer

1.2.1 The human colon

The human large intestine is the last part of the gastrointestinal tract (GIT), which is long, tube through which undigested food is stored prior to defecation (Figure 1.2). It begins from the end of the small intestine to the anal canal (13). There are three sections of the large intestine: colon, rectum, and anus. The colon is further divided into parts. The first part is the cecum, which is the entry point and is 6 inches long. The ascending colon travels up, joining the transverse colon, which in turn joins the descending colon. The colon is wider than the small intestine but is shorter (1.8 meters against 6.7 meters) (14,15). The colon functions as a storage of undigested material and also for defecation (15). The pH of each part of the colon varies slightly, with the ascending colon being 5.4 to 5.9; transverse colon 6.2, descending and sigmoid colons are 6.6 to 6.9 (16). Thus, the overall of the colon is approximately 6.4±0.6 and 7.0±0.7 in the proximal and distal regions respectively (17).

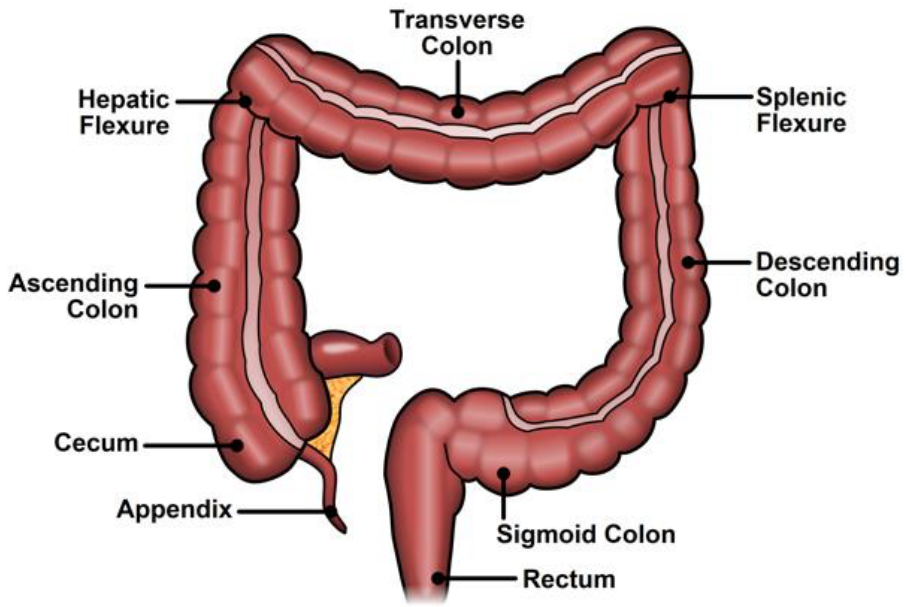

Figure 1.2 Structure of the human colon. Adapted from (16).

1.2.2 Colorectal cancer (CRC)

According to the World Health Organization (WHO), colorectal cancer (CRC) is the third most common cancer in both males and females. In the US, it accounts for 8% of new cancer cases (18). CRC ranks 5th in men and fourth in women with mortality rates still rising (19,20). CRC begins as a benign adenomatous polyp, which evolves to an advanced adenoma with high-grade dysplasia, and finally to an invasive cancer (21). The progression of CRC comprises of four distinct stages. Stage 0 manifests when the cells are still *in situ* and have not spread yet. Stage I involves small cancer cells that have not yet spread. In stage II cancer cells are grown but are not spread. Stage III presents as fully-grown cells that have the ability to spread. Finally, in stage IV, cancer cells are spread to at least another organ, and the cells are referred to "metastatic cancer". In stage 0, I and II, a surgical treatment can be applied to remove the cancer cells from the body before spreading (Figure 1.3) (22,23).

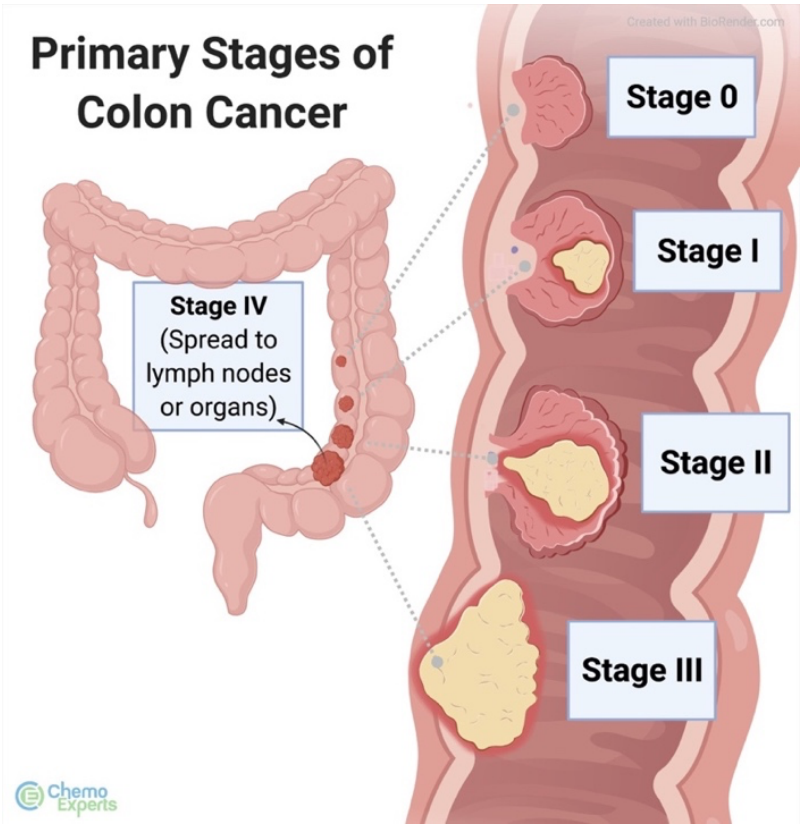

Figure 1.3 Illustration of different stages of colorectal cancer (CRC). Adapted from (23).

There are predisposing factors that increase the chances of developing cancer. For example, a study in Japan, estimated that smoking, alcohol drinking, obesity and overweight, and physical inactivity contributed to 33.6% and 31.7% of colon cases and deaths, respectively (24). Another study concluded that nutritional, occupational, and hormonal factors contributed to death from CRC (24). Symptoms of CRC include consistent changes in the bowel habits such as diarrhea or constipation, or a change in stool consistency, the presence of blood in stool or rectal bleeding, consistent stomach pain, cramps, gas, or bloating, weakness or exhaustion, anemia, decreased appetite, and an unexplained weight loss (25).

Treatment options for CRC include surgical removal of affected parts, radiotherapy, and chemotherapy. Chemotherapy is frequently used as an adjuvant

treatment after surgery. Typical chemotherapeutic agents include capecitabine (Xeloda®), capecitabine (Xeloda®) + oxaliplatin; FOLFIRI + bevacizumab, FOLFIRI + cetuximab (Erbitux®) (26). However as mentioned earlier, the use of these chemotherapeutic agents is associated with severe side effects that may even be life threatening. Hence the need for safer alternatives.

1.3 Curcumin

Curcumin is a yellow powder that derived from turmeric, *Curcuma longa L* (Figure 1.4). The IUPAC name of curcumin is 1,7-bis(4-hydroxy-3-methoxyphenyl)-1,6-heptadiene-3,4-dione (Figure 1.5) (27). It is commonly used as a spice in the Indian cuisine and is used as a traditional Chinese and Indian medicine to treat infections, injuries, stress, depression, and skin diseases (28). It has been shown to have antioxidant, anti-inflammatory, antiviral, antibacterial, antifungal, and anticancer properties. Active research on curcumin also indicates its use in a variety of cancers, diabetes, allergies, arthritis, and Alzheimer's disease (29).

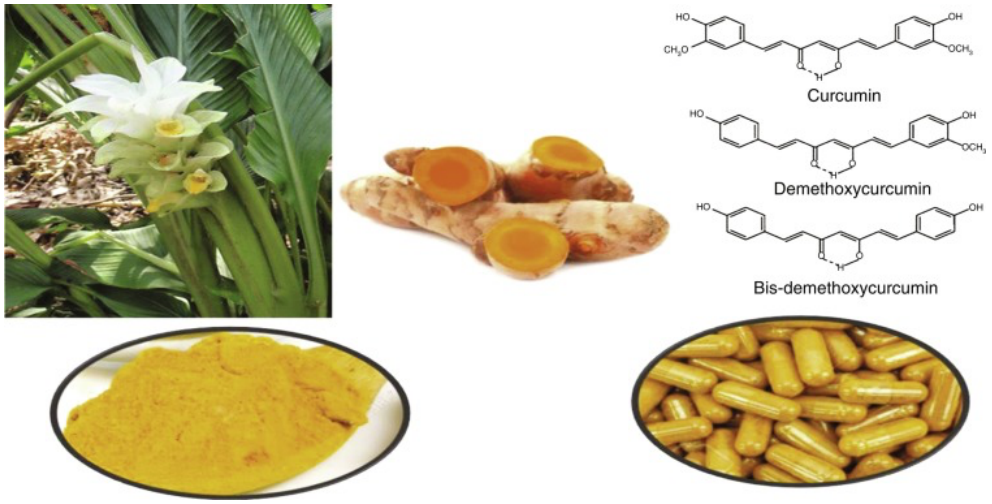

Figure 1.4 Turmeric, Curcuma longa L. Adapted from (29).

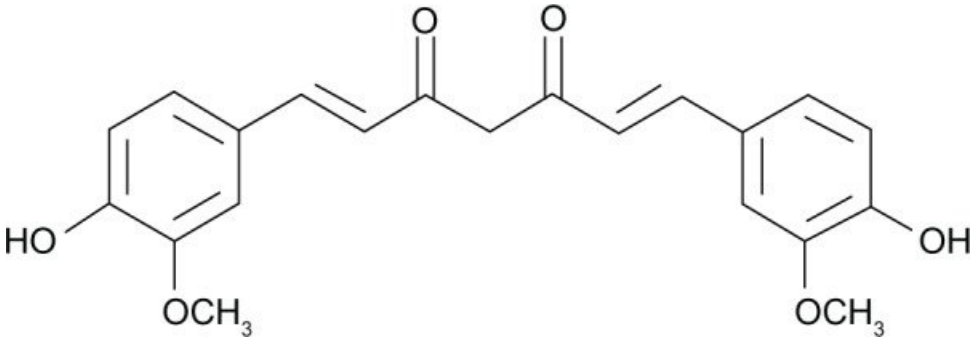

Figure 1.5 Chemical structure of curcumin. Adapted from (30).

1.3.1 Chemical properties of curcumin

Curcumin is a hydrophobic polyphenol with a molecular weight of 368.4 $gmol^{-1}$, density of 0.9348 at 15°C and a melting point of 183°C. Due to its bright yellow color, it is often employed as a dye. It exists in variety of tautomeric forms as shown in Figure 1.6. The aromatic rings are functionalized with methoxy and hydroxy groups on the *ortho* positions of the aromatic rings, which are in turn linked by seven-carbon spacer containing two α, β-unsaturated carbonyl groups (30). It is insoluble in water at neutral and acidic pH, however it dissolves in organic solvents such as dimethyl sulfoxide (DMSO), acetone, ethanol, methanol, and oils. It is also soluble in alkaline and highly acidic solvents, due to the ionization of the phenolic groups (31).

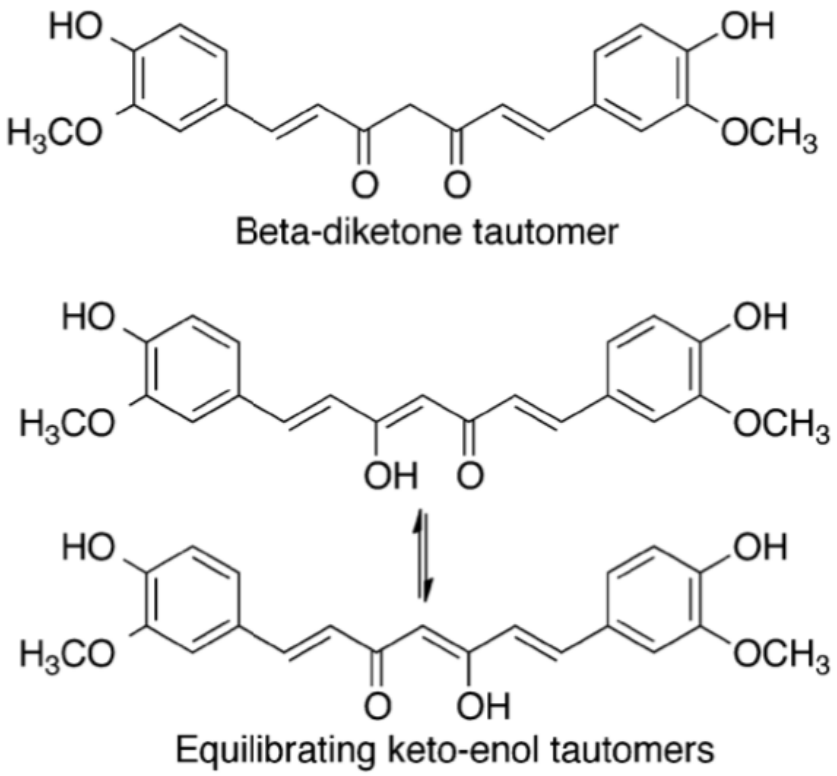

Figure 1.6 Tautomeric forms of Curcumin (31).

1.3.2 Therapeutic properties of curcumin

1.3.2.1 Antioxidant properties

Curcumin has been shown to protect bio-membranes against peroxidative stress (32). Peroxidation of lipids is known to be a free-radical-mediated chain process that causes cell membrane damage, and curcumin's prevention of peroxidation is mostly related to the scavenging of reactive free radicals involved in peroxidation. The majority of antioxidants have a phenolic functional group or a β-diketone group such as curcumin, which is unique with a diverse set of other functional groups (32).

Researchers compared the rate constants of the reaction of 1,1-Diphenyl-2-picrylhydrazyl (DPPH) radical with curcumin in ionizing and nonionizing solvents and resolved the curcumin antioxidant controversy by proposing the mechanism of sequential proton loss electron transfer (SPLET); that is, in solvents that support

ionization, curcumin reacts with electrophilic radicals initially at the ionized keto-enol moiety and the resulting non-ionization. In nonionizing solvents, however, the SPLET mechanism is not possible, and the reactions require H-atom transfer from a phenolic hydroxyl group of the neutral curcumin to the radical (32).

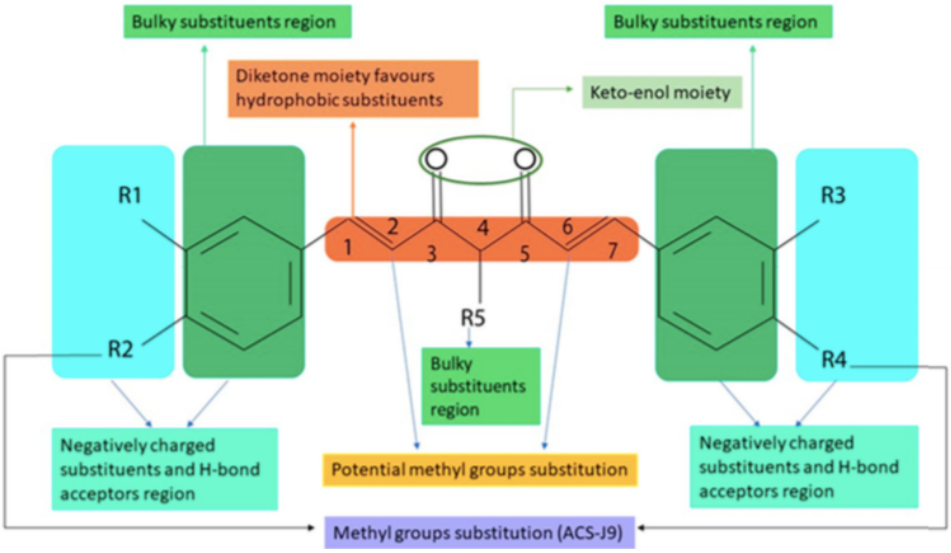

Figure 1.7 The main pharmacophores and potential substitution positions. Adapted from (34).

1.3.2.2 Anti-inflammatory properties

The anti-inflammatory properties of curcumin is comparable to that of steroidal and nonsteroidal medications such as indomethacin and phenylbutazone, both of which pose serious side effects. Its anti-inflammatory properties appear to be mediated via inhibition of cyclooxygenase (COX)-2; a key enzyme that is responsible for the conversion of arachidonic acid to prostaglandins (PG), lipoxygenase (LOX), inducible NOS (iNOS), and synthesis of cytokines such as interferon-and tumor necrosis factor, as well as activation of transcription factors such as NF-B and AP-1 (32).

1.3.3 Mechanism of action against cancer

The mechanism of action of curcumin against cancer progression is via induction of apoptosis and inhibiting the proliferation and invasion of the tumor by suppressing a variety of cellular signaling pathways. Curcumin inhibits the transformation of tumor cells and that it induces cell cycle arrest by downregulating the nuclear factor kappa-B (NF-κB). The NF-κB is a ubiquitous and regulates many genes that are involved in the growth regulation, inflammation, carcinogenesis, and apoptosis of cells. Constitutive activation of NF-κB inhibits chemotherapy-induced apoptosis in a variety of cancer cells, according to in vitro and in vivo investigations (33). Signal transducer and activator of transcription 3 (STAT3) is a widely expressed transcription factor in the STAT family and is activated by tyrosine phosphorylation via upstream receptors such as epidermal growth factor (EGF), platelet-derived growth factor (PDGF), and cytokines such as interleukin-6 (IL-6) (33). STAT3 possess cancer resistance to chemotherapeutic drugs and a significant mediator in carcinogenesis (33). The carcinogenic potential of activated STAT3 molecules stems from their impact on a variety of parameters; including apoptosis, cell proliferation, angiogenesis, and immune system evasion. Active STAT3 has been implicated in the development of apoptosis resistance, most likely via the expression of Bcl-xL and cyclin D1 on of genes that inhibit apoptosis, mediate proliferation, invasion, and angiogenesis (33). Whilst the anticancer effect of curcumin is conceivable, there are limitations to its ability to fully manifest its effects. Through appropriate formulation strategies, it is possible to surmount these limitations and harness the full potential of curcumin. This means that a lesser drug load will be required through formulation which translates to potentially reduced side effects as well. In the following section we discuss relevant nano-formulations that have been used in this regard.

1.3.4 Curcumin nano-formulations

Over the past few years, curcumin has been extensively studied for its powerful anticancer effects and several curcumin nano-formulations have emerged in an attempt address its poor solubility and bioavailability (34,35). Most of the formulation approaches focused of improving the bioavailability and solubility of curcumin (36). Encapsulation of curcumin in nano-formulations includes liposomes, cyclodextrin in micelles, and curcumin's nanospheres and microspheres (37). Curcumin silk fibroin (CUR-SF) nanoparticles were more stable than free curcumin and showed better uptake by HCT116 cell lines, consequently manifesting stronger anticancer effect (36). A one-step solid dispersion approach of curcumin encapsulated polymeric micelles (Cur-M) was shown to be effective on breast tumor (36).

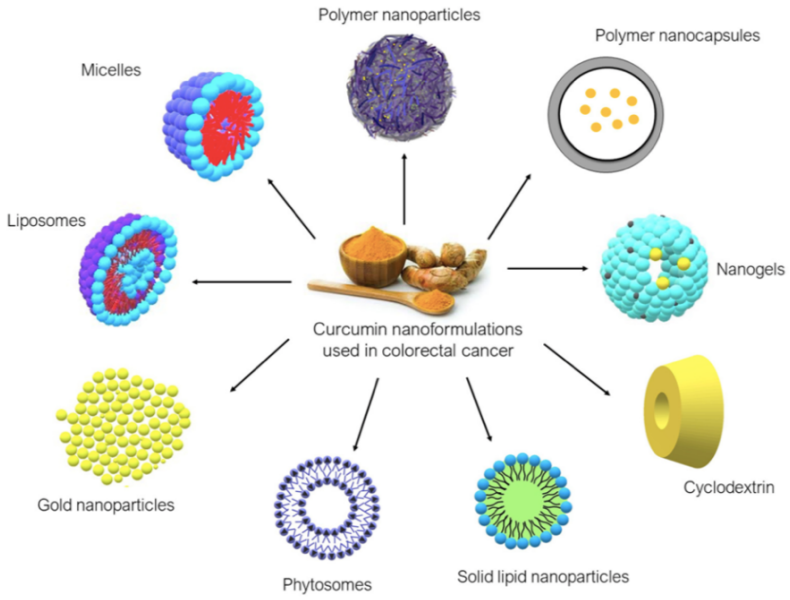

Figure 1.8 Possible curcumin nano-formulations used in colorectal cancer (37).

1.4 Modified citrus pectin

Pectin is a soluble fiber found in the peel and pulp of citrus fruits and is a complex polysaccharide (38,39). It is commonly used for cholesterol lowering effect, typically low-density lipoprotein (LDL) (40). It is safe for human consumption when taken in moderate amounts (41).

Despite the wide availability of chemotherapeutic agents for use in CRC, most present several side effects to patients, thus it is important to focus on effective agents that present fewer effects (42). According to previous studies, it was found that CRC metastatic cells can be suppressed using naturally found components such as citrus pectin (43). Based on preliminary studies, it was found that by modifying citrus pectin, absorption can be enhanced leading to improved bioavailability and bioactivity (40). MCP has chemo-preventive and anti-cancer activities on aggressive cancers, such as prostate cancer, breast cancer and CRC (38).It inhibits tumor growth, reduce the tumor metastasis, and promote the apoptosis (38). This potency correlates lower degrees of esterification (DE) in MCP compared to native pectin(38). Studies have shown that the galectin moiety in MCP has antagonistic specificity to the metastatic and tumor cascade involved in the development of CRC (44,45). Nano-formulation has emerged as an effective option to deliver drugs in cancer therapy (42). In this regard, MCP, when formulated as nanoparticles, would serve as a promising strategy for CRC therapy.

In order to improve the yield of galectin moieties on MCP, several techniques have been proposed including modification by pH (5), modification by thermal treatment (46,48). MCP is a potent galectin-3 inhibitor, where high concentrations of galectin-3 are commonly found circulating in the blood of patients suffering from different types of cancers (45). Recent studies showed that by reducing the galectin-3

blood levels using MCP, it is possible to significantly prevent the spread of the cancer cells (45,46).

1.4.1 Moieties responsible for anti-colon cancer effect in MCP

Chemically, galectin rich MCP is formed through chemical processes such as exposure to alkaline pH (pH 10), exposure at elevated temperatures for several hours followed by acid treatment at room temperature (47,48). This chemical treatment has been reported to influence the galectin yield on MCP and hence the anti-cancer properties (49).

The chemical structure of MCP is shown in Figure 1.9, as proposed by Hait (54). Three central pectic polysaccharides are recognized namely: homogalacturonan (HG), rhamnogalacturonan-I (RG-I) and the substituted galacturonans (GS) with an average percentage of 65%, 20-35% and 10%, respectively. The linear HG regions permeated by the RG-I zones; therefore, they are substituted by the neutral sugars as side chains (51).

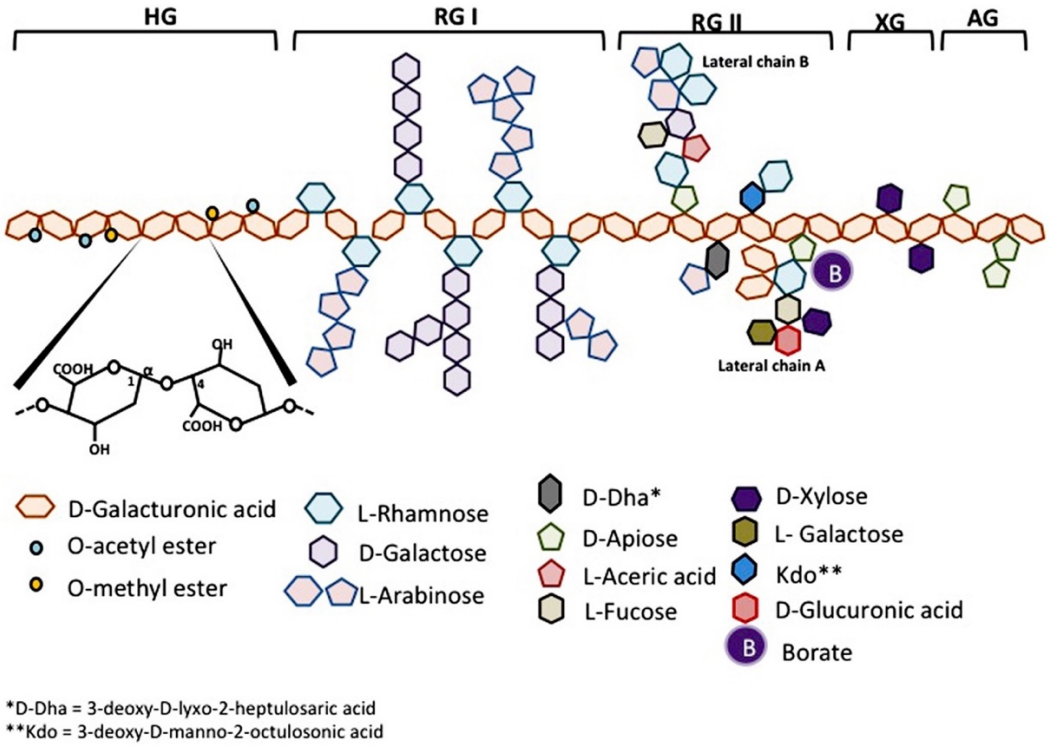

Figure 1.9 Proposed structure of MCP. Adapted from (54).

Furthermore, in cancer metastasis, tumor cell arresting in distant organs is the rate-limiting step shown in Figure 1.10 (53). The interaction of Gal-3 with cancer-associated Thomsen-Friedenreich glycoantigen, mediates the initial adhesion of the cancer cells to the vascular wall (53). The anti-adhesive property of MCP was found to be effective as anti-metastatic (40,54). The use of MCP in conjunction with curcumin appear to be a rational and safer approach to treating CRC, whereby MCP serves a dual purpose of encapsulating curcumin within the nanoparticles and preventing premature release in the upper GIT acidic pH, whilst also providing the galactose moiety which inhibits (Gal-3) (49).

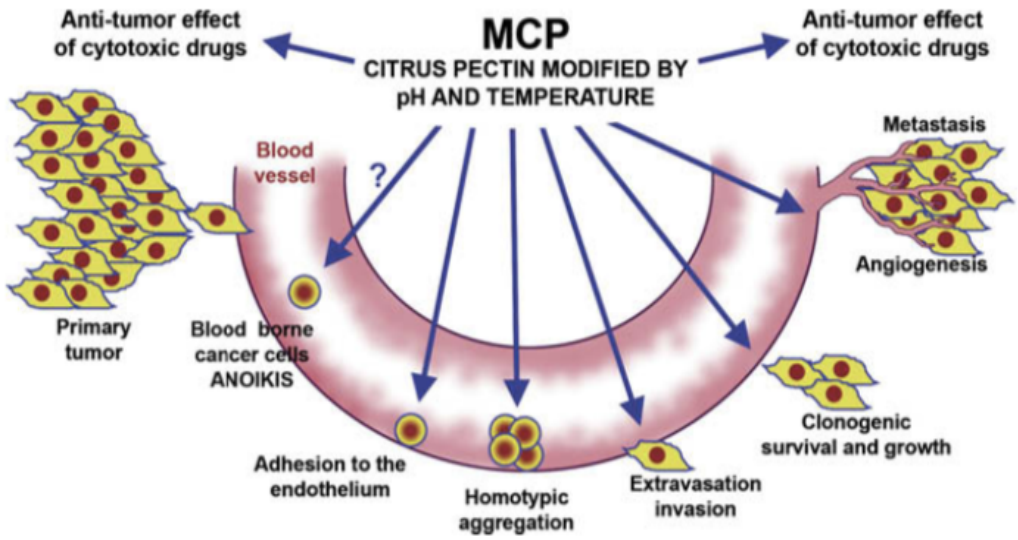

Figure 1.10 Cancer metastasis rate-limiting step which is targeted by MCP. Adapted from (47).

Tumor cells can either spread intravascularly, (followed by metastatic tumor growth outside the blood vessels that invades organ parenchyma) or may extravasate before initiating a secondary tumor growth (53). Extravasation depends on the invasive propensity of the cancer cells and involves a series of tumor cell interactions with the extra-cellular matrix (ECM) proteins (53). Likewise, MCP is capable of inhibiting the Gal-3-mediated tumor cell interactions efficiently with ECM proteins (53). Based on constructed results, it is shown that the *in vivo* effects of MCP on experimental metastasis involves an inhibition of the tumor cell invasions (53).

Most common anticancer drugs induce tumor cell apoptosis through intrinsic (mitochondrial) apoptosis pathway. Gal-3 as an important cancer cell apoptosis regulator, plays an important role in suppressing the mitochondrial apoptosis pathway (53). In addition, Gal-3, has a direct sensitivity to cancer cells after exposure of the cells to several chemotherapeutic agents such as cisplatin and dexamethasone, thus MCP can potentially change the cancer cells sensitivity toward the cytotoxic drugs (53).

1.4.2 Citrus pectin modification methods

There are several methods for chemically modifying citrus pectin. Thermal alkaline modification that involves the exposure to of native pectin to alkaline pH at high temperature (60ºC) followed by neutralization and washing (49). Furthermore, native pectin can be treated on microfluidizer at very high pressure (20,000 psi) (55). Ultrasonication at very high frequency (20 kHz, 750 W) in cycles was also performed as a modifying method of MCP. UV/H_2O_2 oxidation in acidic and basic conditions can be performed for up to 5 hours under different H_2O_2 concentrations (55). Figure 1.11 represents the preparation of MCP fragments flow chart.

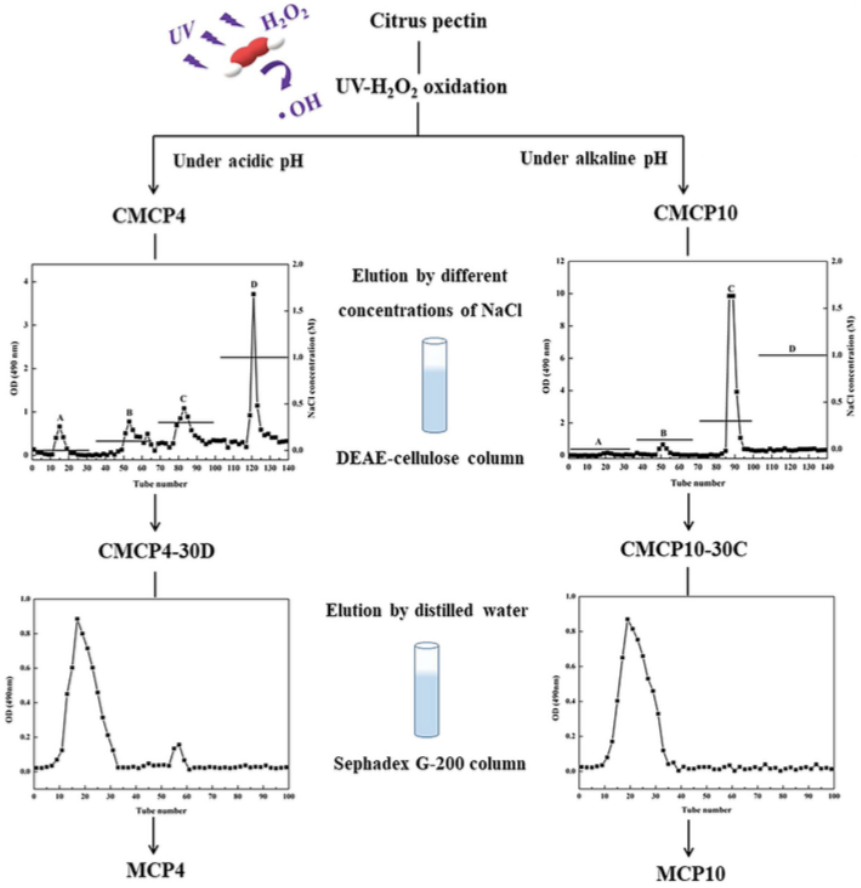

Figure 1.11 Preparation and purification of MCP fragments flow chart. Adapted from (39).

1.5 Chitosan

Development of colloidal systems for encapsulation and delivery of curcumin has been explored in overcoming some of the limitations associated with physical properties of curcumin (56). Biopolymeric nanoscale delivery systems such as chitosan, pectin, cellulose etc are effective as anticancer delivery systems due to their biocompatibility, biodegradability, and non-toxic characteristics (56). Chitosan is a linear polysaccharide comprised of repeated units of β-(1-4)-linked D-glucosamine and N-acetyl-D-glucosamine (Figure 1.13) and is obtained from exoskeletons of marine crustaceans such as crabs, shrimps, lobsters, prawns, and fungi (57,58). The presence of an amino group at the C-2 position of the polysaccharide glucosamine (59), improves its functional and structural characteristics. For example, the amino group symbolizes its cationic nature and confers innate wound healing, antibacterial action, and muco-adhesiveness, making it a useful drug delivery system (59). It has a pKa of 6.5 and is soluble in acidic solutions but insoluble in water (60). It is protonated and polycationic in nature, forming complexes with a variety of anions such as lipids, proteins, DNA, alginate, pectin, and polysaccharides (acrylic acid) (59).

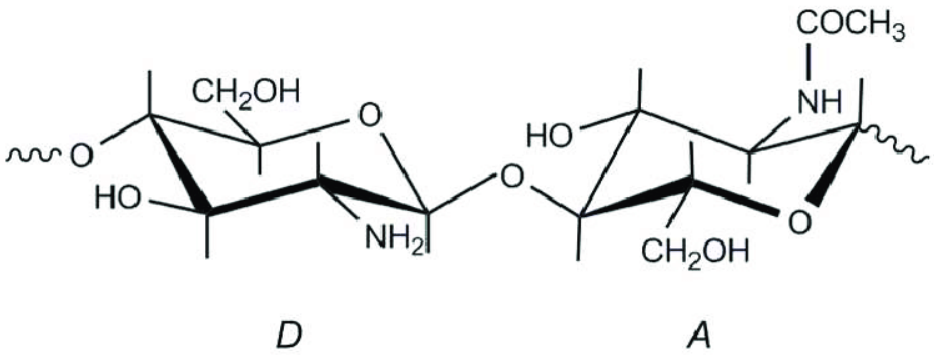

Figure 1.12 Structural units of chitosan. (A) N-acetyl-D-glucosamine; (D) Glucosamine unit. Adapted from (53).

1.6 Nanomedicine

The term ‘nanotechnology’ was coined by Richard P. Feynman in 1959, during his famous lecture “*There’s Plenty of Room at the Bottom*”. However, nanotechnology has evolved significantly since the last century and is now defined as the science of materials of various types at a nanoscale level (61). Nanotechnology has been introduced into our daily lives in recent years. Using an integrated approach, this innovative technology has been implemented in a variety of sectors. The use of nanotechnology in the creation of novel medicines has been designated as a key enabling technology and is capable of bringing new and creative medical solutions to meet unmet medical needs (62). Medical nanotechnology deals with the application of nanotechnology for medical reasons, and it is described as the use of nanoparticles for illness diagnosis, monitoring, control, prevention, and therapy (62).

1.6.1 Types of Nanocarriers

Several types of nanocarriers have been proposed for use in cancer therapy, and they are typically customized to their roles. Based on the therapeutic substances to be delivered, the nanocarriers can be tailored for systemic or local administration, burst, extended, or targeted release can be obtained through careful section of the right material or processing variables (63). Lipids, polymers, and inorganic materials such as gold and iron oxide can be employed to construct nano-sized drug delivery systems. Polymeric nanoparticles (NP), micelles, liposomes, dendrimers, and lipid-based NP are the most frequent forms of nanocarriers. Every system has specific physicochemical features that result in diverse in vitro and in vivo behavior, as well as distinct benefits and drawbacks (63).

1.6.2 Challenges in nanomedicine

Nanomedicine imposes several challenges in the transition from bench to market and these challenges needs to be overcome to deliver a safe and effective active

pharmaceutical ingredient to patients. Such challenges are realized during the development of nanomedicine, including physicochemical characterizations, biocompatibility, nanotoxicology evaluation, pharmacokinetics and pharmacodynamic assessment, process control, and up-scale-reproducibility (62). Physicochemical characterizations of nanomedicine are required to understand its activity in human body and to provide guidance for process control and safety evaluation (67). Another problem in nano-pharmaceutical development is controlling the production process parameters by identifying essential characteristics and the tools needed to analyze them. New techniques have emerged as a result of pharmaceutical innovation and regulatory agencies concerns about the quality and safety of new drugs (68). One of the pharmaceutical development methodologies known for the systematic assessment and control of nanomedicines is Quality-by-Design (QbD), which is backed by Process Analytical Technologies (PAT) (69). It should be noted that certain of the physicochemical properties of nanoparticles might change throughout the production process, compromising the quality and safety of the final nanomedicine (70).

1.7 Aims and objectives

The anticancer properties of curcumin have been discussed earlier in the thesis, including promising outcomes in the treatment of colorectal cancer. However, as mentioned earlier, the full potential of curcumin cannot be realized unless some formulation or chemical intervention is adapted. We note the usefulness of MCP in treating colon cancer and being able to prevent premature release of the drug cargo when formulated in nanoparticles. We note that curcumin in nanoparticles has been used as a means to effectively deliver curcumin to colon cancer cells. Finally, we note that chitosan possesses mucoadhesive properties. Packaging these strands together, the main objective of this work is to formulate a curcumin in chitosan-MCP nanoparticles,

that can deliver curcumin to the colon where it manifests its action locally. We believe this arrangement is likely to manifest more effective anticolon cancer effects, possibly free from side effects observable with chemotherapeutics.

Specific objectives include:

- Improve the galectin yield on citrus pectin
- Encapsulate curcumin in a chitosan MCP nanoparticulate system
- Characterize the above delivery system
- Study the anti-colon cancer effects of the delivery system on cancer cell lines

CHAPTER 2: FORMULATION AND CHARACTERIZATION OF CURCUMIN IN CHITOSAN-MCP NANOPARTICLES

2.1 Materials

Table 2.1: Materials and Chemicals

Materials	Supplier
Acetic Acid Glacial (<99%)	Fisher Scientific
Acetic acid	Honeywell Fluka
Acetonitrile (>99.9%)	Fisher Scientific
Acetone (>99%)	Honeywell Fluka
AlamarBlue	ThermoFisher
Citrus Pectin	Alfa Aesar
Curcumin (98%)	Acros Organics
Chitosan	Acros Organics
Dimethyl Sulfoxide (ACS reagent) (>=99.9%) (DMSO)	Sigma Aldirch
Dulbecco's Modified Eagle Medium (DMEM)	ThermoFisher
Ethanol (>99.8%)	Honeywell Fluka
Fetal Bovine Serum (FBS)	ThermoFisher
Methanol (>99.9%)	Honeywell Fluka
Phosphate-Buffered Saline (PBS) pH 7.4	ThermoFisher
Trypan Blue	ThermoFisher
Trypsin EDTA	ThermoFisher
Sodium Tripolyphosphate (Granular)	Alfa Aesar

2.2 Calibration curves

Stock solution of curcumin in methanol was used to construct a calibration curve (0.005 to 0.03 mg/mL). The standard curve was used to estimate the amount of curcumin in the nanoparticles and in release studies.

2.3 Determination of curcumin content

A reversed phase high performance liquid chromatographic system (HPLC) was used to determine the concentration/amount of curcumin in nanoparticles, release studies and where necessary. The HPLC comprised of a Series 1269 quaternary pump, Agilent, USA operated at 0.3 mL/min. The mobile phase was comprised of methanol, acetic acid, and acetonitrile (5%:57%:38%) respectively, and detection was by UV detection at 425 nm.

2.4 Modification of citrus pectin

Modification of citrus pectin was done according to (64), with slight modification. Briefly, 1.5 g of citrus pectin (CP) was added in 100 mL of ultra-pure water in three 250 mL beakers. The pH was adjusted to 10 with 3M of NaOH and stirred at 60^{o}C for 1h, 2h, or 4h, and then cooled to room temperature. The pH of each formulation was adjusted to 3 using 3M HCl and then stored at 4^{o}C overnight. 30 mL of 95% ethanol was added to each beaker and then centrifuged at 2000 rpm for 10 min. The content was transferred to petri dishes and dried in the oven overnight at 50^{o}C overnight. The MCP were labeled based on the stirring duration of stirring: 1, 2, and 4 hrs as MCP1, MCP2, and MCP4 respectively.

2.5 Formulation of MCP-NPs and CCM-NPs

To prepare CCM-NPs, curcumin was dissolved in ethanol at 1 mg/mL, whilst chitosan (CS) was dissolved in 2% v/v acetic acid at 0.5 mg/mL and the pH of the solution was adjusted to 5 with 2M NaOH. STPP was dissolved in ultra-pure water at 0.5 mg/mL and pH was adjusted to 2 with 2M HCl. MCP was dissolved it in ultra-pure

water at 0.5 mg/mL followed by sonication for 30 minutes to dissolve completely. A series of formulations were prepared by adding amounts indicated in Tables 2.1-2.5 of MCP was added to an Eppendorf, followed by the addition of curcumin dropwise. Then chitosan solution was added dropwise to the same tubes, followed by dropwise addition of STPP. The complexation between the opposite charged molecules caused the formation of the spherical nanoparticles by ionic gelation (65). The NP suspensions were centrifuged for 20 min at 16000 xg and the supernatants discarded, and the pellet was re-suspended in 1 mL of ultra-pure water and re-centrifuged at 16000 xg for 20 min. The prepared samples were freeze dried for further analysis.

The control nanoparticles (MCP-NPs) were prepared similarly without the addition of curcumin. Each MCP formulation (MCP1, MCP2, and MCP4) were prepared as nanoparticles. Tables 2.1, 2.2, 2.3, 2.4, and 2.5 below shows the different composition of each formulation prepared.

Table 2.2: STPP concentrations at 0.5mg/mL each of MCP and CS used for MCP-NPs formulations (MCP1, MCP2, and MCP4).

MCP formulation	STPP concertation (mg/mL)
STPP-MCP1-NPS	0.5
STPP-MCP1-NPS	0.7
STPP-MCP1-NPS	1.0
STPP-MCP2-NPS	0.5
STPP-MCP2-NPS	0.7
STPP-MCP2-NPS	1.0
STPP-MCP4-NPS	0.5
STPP-MCP4-NPS	0.7
STPP-MCP4-NPS	1.0

Table 2.3: CS concentrations at 0.5mg/mL each of MCP and STPP for MCP-NPs formulations (MCP1, MCP2, and MCP4).

MCP formulation	CS concentration (mg/mL)
CS-MCP1-NPS	0.5
CS-MCP1-NPS	0.7
CS-MCP1-NPS	1.0
CS-MCP2-NPS	0.5
CS-MCP2-NPS	0.7
CS-MCP2-NPS	1.0
CS-MCP4-NPS	0.5
CS-MCP4-NPS	0.7
CS-MCP4-NPS	1.0

Table 2.4: Volumes of CUR, MCP, and CS used at varying amounts of STPP for formulating CCM-NPs.

Formulation	CUR amount (μL)	MCP amount (μL)	CS amount (μL)	STPP amount (μL)
1AC	300	500	600	300
1BC	300	500	600	400
1CC	300	500	600	500

Table 2.5: Volumes of CUR, MCP, and STPP used at varying amounts of CS for formulating CCM-NPs.

Formulation	CUR amount (μL)	MCP amount (μL)	CS amount (μL)	STPP amount (μL)
2AC	300	500	600	300
2BC	300	500	700	300
2CC	300	500	800	300

Table 2.6: Volumes of MCP, CS, and STPP used at varying amounts of CUR for formulating CCM-NPs.

Formulation	CUR amount (μL)	MCP amount (μL)	CS amount (μL)	STPP amount (μL)
3AC	100	500	600	300
3BC	200	500	600	300
3CC	300	500	600	300
3DC	400	500	600	300

2.6 Size and zeta potential analyses

The average size of the formulated nanoparticles was measured using fresh samples where the supernatant was separated from the pellet after centrifugation, and 900 μL transferred to the cuvettes of a laser Doppler anemometry (Malvern Instrument zeta sizer, UK) for the size (nm) and a capillary cuvette for the zeta potential (mV). Each measurement was done in triplicate and the data were expressed as mean $\pm$ standard deviation (SD).

2.7 X-ray diffraction analysis (XRD)

XRD analysis was performed using X-ray diffractometer (X-ray diffractometer, PANalytical, Netherlands). The analysis was performed after mounting samples on the platform and operating the X-ray source moves at 2θ values from 5^{o} to 75^{o} with scanning speed of 0.02^{o}/step and the step time was 0.5s.

2.8 Fourier transform infrared (FT-IR)

The FT-IR spectra of samples were obtained by adding the samples on KBr using the FT-IR spectrometer Vertex 70 (FTIR Spectrophotometer, Perkin Elmer, USA). 100 μL of sample was put on 20 mg of KBr and was kept to air dry at room temperature overnight for the FT-IR analysis. Lastly, the spectra will be read in the range of 4000 to 400 cm^{-1} at 4 cm^{-1} resolutions.

2.9 Scanning electron microscopy (SEM)

A drop of nanoparticle suspension was placed on the SEM imaging stub and left to air dry at room temperature before mounting on a Scanning Electron Microscope (SEM) (Model Nova Nano SEM 450, ThermoFisher Company) and operated at 5KV.

2.10 Atomic force microscopy (AFM)

For the AFM preparation, a drop of each sample was placed on a clean mica sheet and was air-dried overnight at room temperature. The dried samples were placed on the platform of the microscope and scanned using the tapping mode, with a silicon tip and a spring constant of 0.7 N/m and at a frequency of 150kHz over an area of 5x5 μ (66).

2.11 Thermogravimetric analysis (TGA)

The thermal stability of CCM-NPs was evaluated by thermogravimetric curves (TGA) in Simultaneous Thermal Analyzer (TGA 4000, PerkinElmer, USA). The operating conditions were temperature in the range of 25 to 500ºC, with a heating rate of 10ºC/min and a gentle stream of nitrogen at a flow rate of 50 mL/min.

2.12 Determination of encapsulation efficiency

To quantify the amount of curcumin in the nanoparticles, a standard curve was constructed as stated in section 2.2. The amount of curcumin encapsulated in CCM-NPs was calculated using the following equation:

$$\%\text{Encapsulation efficiency} = \frac{Total\ curcumin\ added - unbound\ curcumin}{Total\ curcumin\ added} \times 100\% \quad \text{(Eq.2.1)}$$

2.13 Curcumin stability test as a function of light

A stock solution of curcumin was prepared by dissolving 5 mg of curcumin in 20 ml of methanol. The curcumin sample was divided into three parts, each part was exposed to different lighting condition: to room light, sun light or in dark, for 0, 30, 60, 120, 240, and 360 min. At the end of each time, 10 μL of each sample was injected on

the HPLC system (HPLC system Series 1260 quaternary pump, Agilent, USA) and peak heights were compared with those from the standard curve in order to determine the concentration of curcumin.

2.14 Curcumin stability in the prepared NPs due after storage

To determine the stability of curcumin in the prepared nanoparticles, two samples of CCM-NPs were stored at 4°C or 37°C for (0, 1, 7, and 14 days) and the samples size, zeta-potential, and PDI were determined for each sample at different durations.

2.15 Drug release

The nanoparticles were prepared as mentioned in section 2.4 and the supernatant transferred to a pooled beaker (total of 7 mL) followed by the addition of 3.5 mL of PBS (pH = 6.8). After gently mixing, 500 μL of the mixture was transferred to seven Eppendorf tubes and the samples were incubated at 37°C in the incubated shaker (Incubated Shaker, Lab Companion, Korea) operated at 150 rpm, at predetermined intervals (0, 1, 4, 6, 24, 48, and 72 hrs) one tube was withdrawn and the samples were centrifuged at 14,000 rpm for 7 mins and then filtered using nylon syringe filters followed by injection of 10 μL on the HPLC to analyze the curcumin content in sample. The reported values are expressed on the mean of three independent runs. The percentage of drug release was calculated according to the following equation:

$$\text{Drug release\%} = \frac{Amount\ of\ curcumin\ released}{Total\ curcumin\ in\ CCM-NPs} \times 100\% \qquad \text{(Eq.2.2)}$$

2.16 Maintenance of cell culture

Human colorectal cell line HCT-116 (American Type Culture Collection (ATCC)) was grown under standard cell culture conditions in Dulbecco's Modified

Eagle Medium (DMEM) with 10% FBS under standard cell conditions of 37°C and 5% CO_2.

2.17 Subculture of cells

The old media was discarded, then the flask was washed with 8 mL of 1x PBS, then it was then removed. 1.5 mL of trypsin was then added to detach the cells and the flask was incubated for 2-5 minutes at 37°C and 5% CO_2. After incubation, the cells were viewed under the microscope (Lecia SP8 UV/Visible inverted microscope) to ensure that the cells are detached. Then, 2 mL of fresh media (DMEM) was added to a 15 mL tube and the total content from the flask was added to the same 15 mL. The tube was centrifuged at 1000 rpm for 5 minutes. Finally, the supernatant was discarded, and the cell pellet re-suspended with 2-3 mL of fresh media.

2.18 Cell counting and seeding

A hemocytometer was used to count the cells after adding 10 μL of the cells mixed with 10 μL of trypan blue in the counting chamber with a coverslip. The chamber was then viewed under the microscope (Lecia SP8 UV/Visible inverted microscope) with a 10X objective. The cells that were in the large central gridded square ($1mm^2$) (Figure 2.1) were counted, while the dead cells that were strained by trypan blue were excluded. The counting was repeated on the opposite side of the hemocytometer. The total number of cells counted was considered by taking the average of both sides of the hemocytometer to obtain the number of cells that are in $1mm^2$. Then, 5000 cells were seeded in each 96-well plate for the needed experiment. The total number of cells was calculated with the following formula:

Total number of cells = average cells per mL x dilution factor of trypan blue x 10^4 (Eq.2.3)

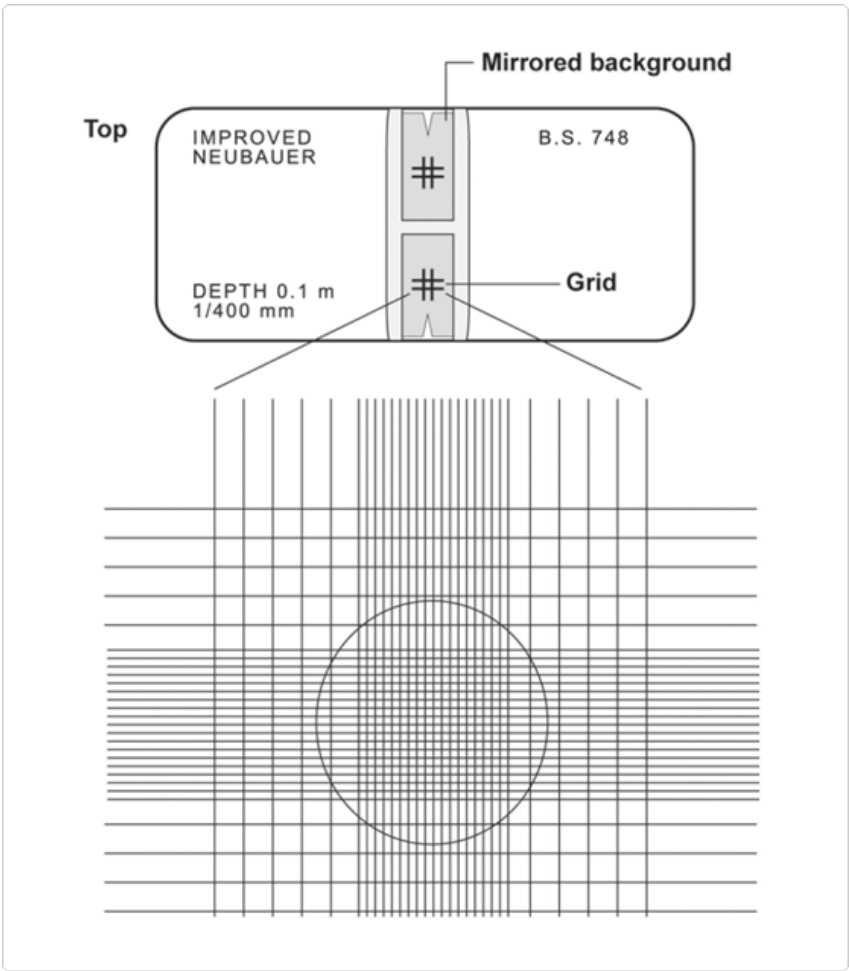

Figure 2.1 A Neubauer hemocytometer (Invitrogen, 2012).

2.19 Cell viability assay

Cell viability (alamarBlue) assay was carried out to determine the effect of CCM-NPs, MCP or free curcumin on HCT-116 cells (67). The cells were initially seeded in three 96-well plates and allowed to attach for 24 hours. On the day of treatment, stock solutions of curcumin, MCP1, MCP2, MCP4, and CCM-NPs were prepared (5μg/mL) in DMSO. The three 96-well plates were labeled as 24h-, 48h-, and 72h-well plate according to the culturing time point. In the 24h-well plate, the culture media was removed and replaced with each treatment according to each determination test: i) determination of IC_{50} of free curcumin after 24, 48, and 72 hours, ii) determination of IC_{50} of MCP1, MCP2, and MCP4's after 24, 48, and 72 hours, and iii)

cell viability of free curcumin compared to CCM-NPs after 24, and 48 hours. To determine the IC_{50} of free curcumin, 2, 2.5, 5, 10, and 15 μg/mL were used. For MCP1, MCP2 and MCP4 determination test, 10, 20, and 40 μg/mL were used. To compare between the anticancer effect of free curcumin and CCM-NPs, the treatment of each group was adjusted to (0.005 μg/mL). At each time point, a mixture of alamarBlue and fresh media was added to each well, and the plate was incubated for four hours at 37^{o}C and 5% CO_2 level. After incubation, the fluorescence from the plates was measured by Infinite M200, TECAN, Austria fluorimeter. Results were expressed as mean$\pm$SD (n=8).

2.20 Statistical analysis

All values were expressed as mean ± SD. Statistical significance was determined by one-way ANOVA as appropriate by using SPSS Software. A difference of p-values < 0.05 was considered statistically significant.

CHAPTER 3: RESULTS

3.1 Size and zeta potential analyses of MCP-NPs and CCM-NPs

During the modification of CP, the effect of stirring rate on measured parameters of the nano-formulations were investigated. The MCP samples were labelled MCP1, MCP2, and MCP4. After modification, these MCP were used to formulate MCP-NPs and CCM-NPs by ionic gelation as described previously in chapter 2.

The variation of STPP (Figure 3.1) concentration (0.5, 0.7, and 1 mg/mL) on MCP-NPs (MCP1, MCP2, and MCP4) were studied and the measured parameters are presented in Figures 3.1 and 3.2.

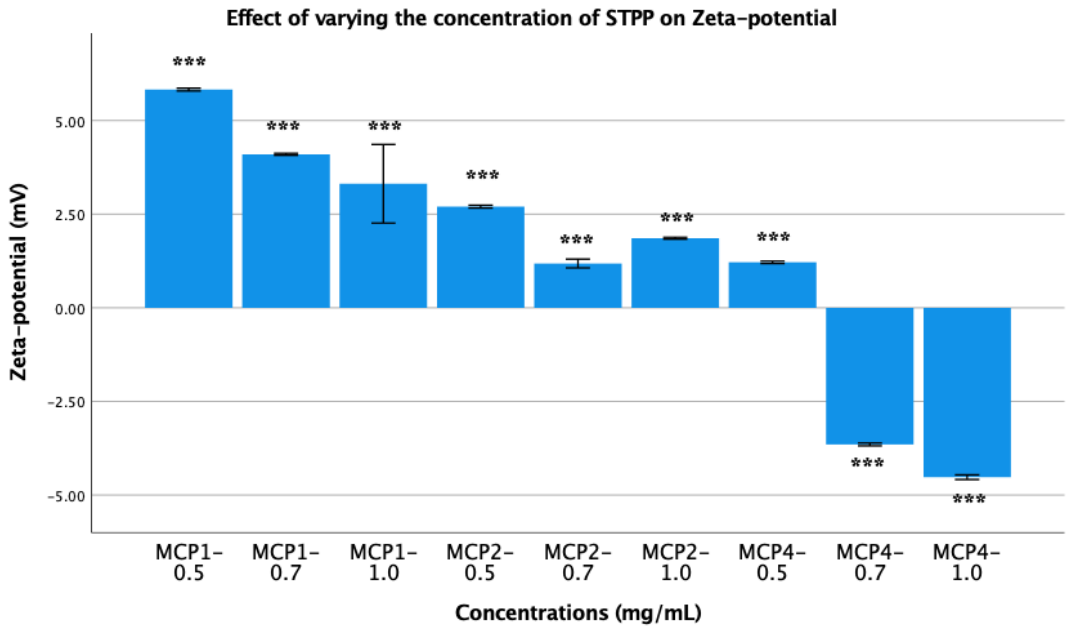

Figure 3.1 Effect of varying the concentration of STPP added on MCP-NPs on Zeta-potential (mV) (*** P<0.001).

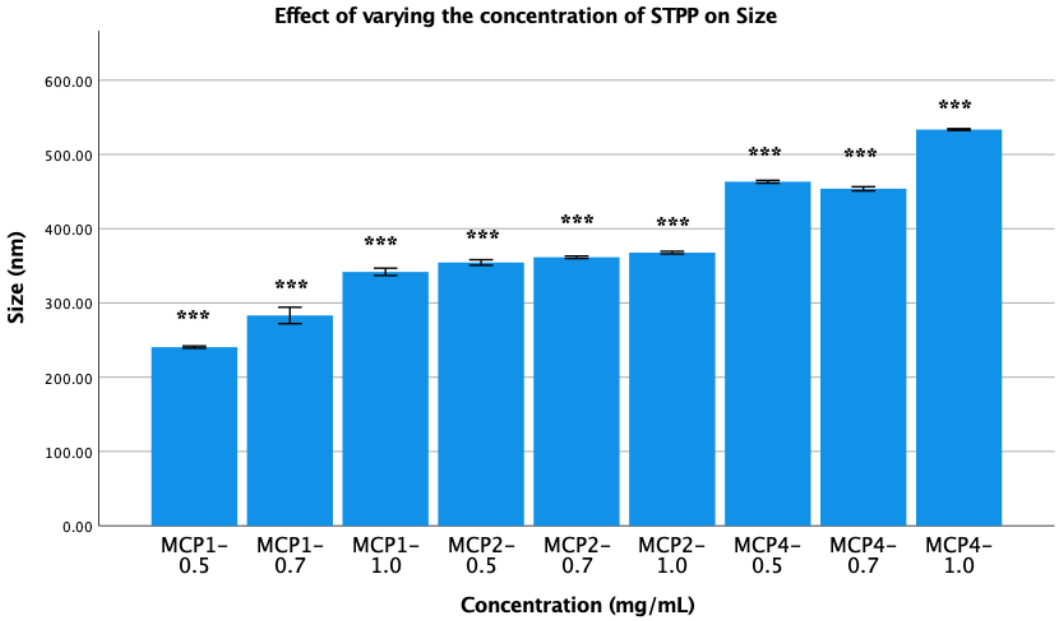

Figure 3.2 Effect of varying the concentration of STPP added on MCP-NPs on Size (nm) (*** P<0.001).

Secondly, the concentration of CS was varied on MCP-NPs, and Figures 3.3 and 3.4 expresses the size and zeta-potential of each formulation.

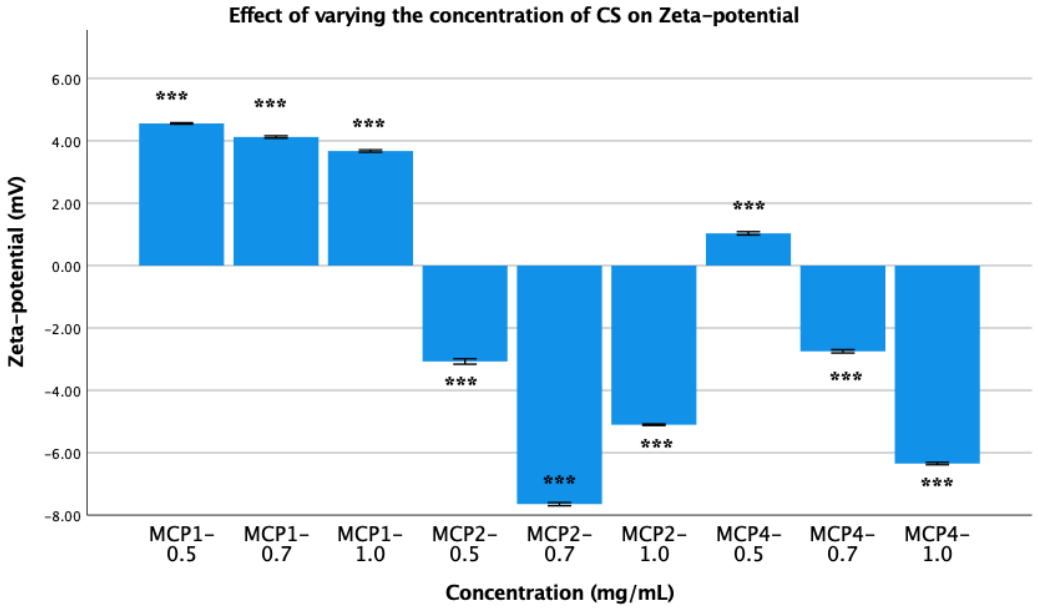

Figure 3.3 Effect of varying the concentration of CS added on MCP-NPs on Zeta-potential (mV) (*** P<0.001).

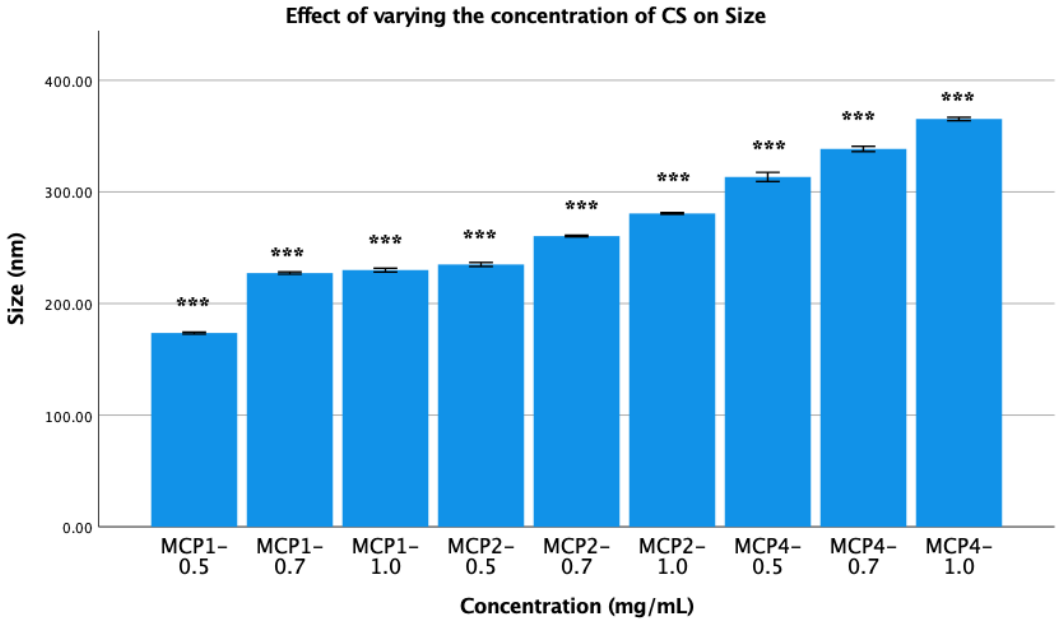

Figure 3.4 Effect of varying the concentration of CS added on MCP-NPs on Size (nm) (*** P<0.001).

The amounts of STPP (300, 400, and 500 μL) and CS (600, 700, and 800 μL) were varied on CCM-NPs, and Figures 3.5-3.8 expresses the size and zeta-potential of each formulation.

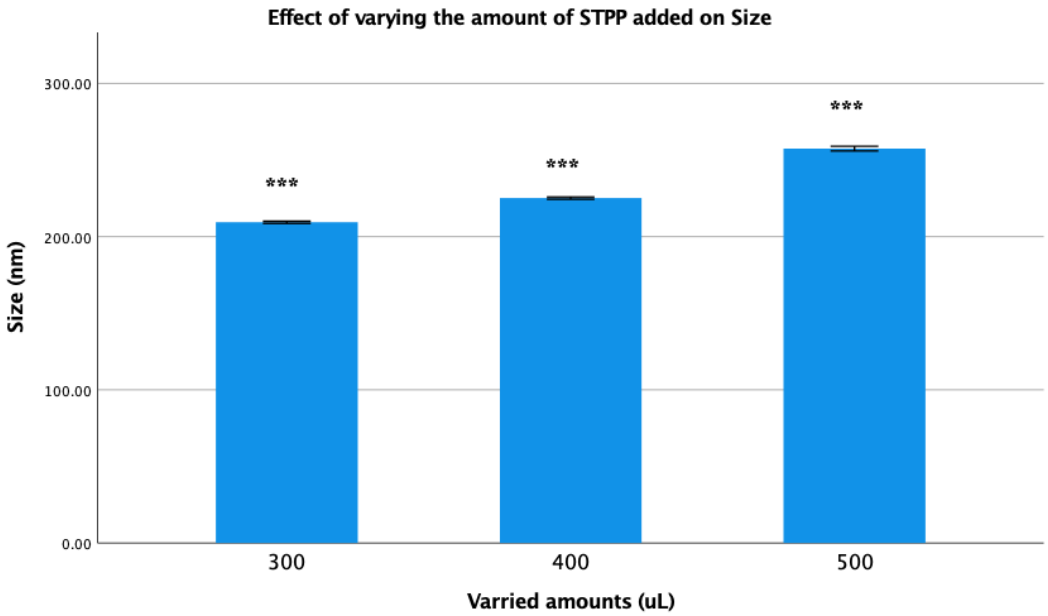

Figure 3.5 Effect of varying the amount of STPP added on CCM-NPs on Size (nm) (*** P<0.001).

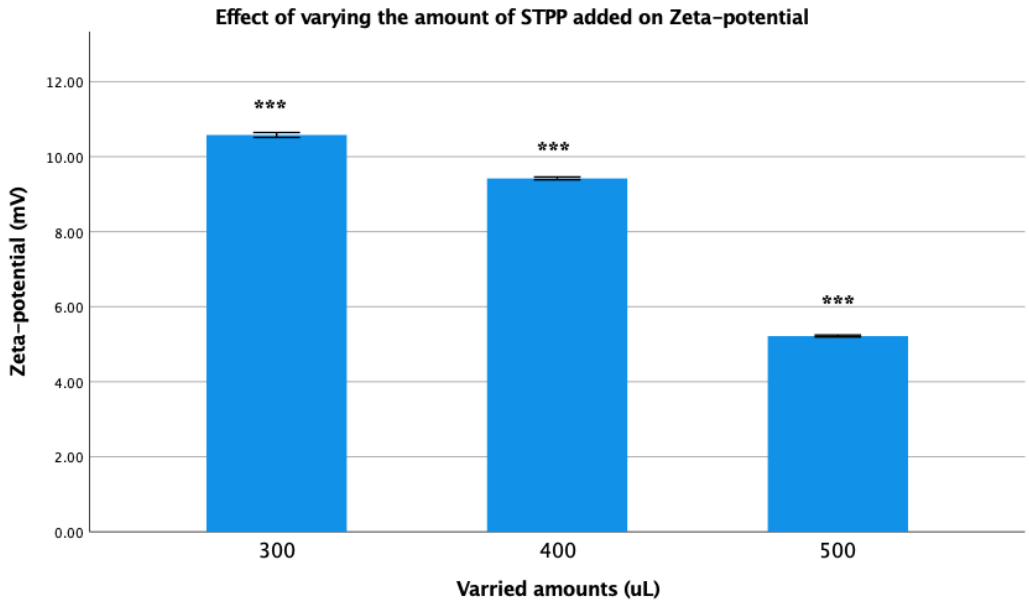

Figure 3.6 Effect of varying the amount of STPP added on CCM-NPs on Zeta-potential (mV) (*** P<0.001).

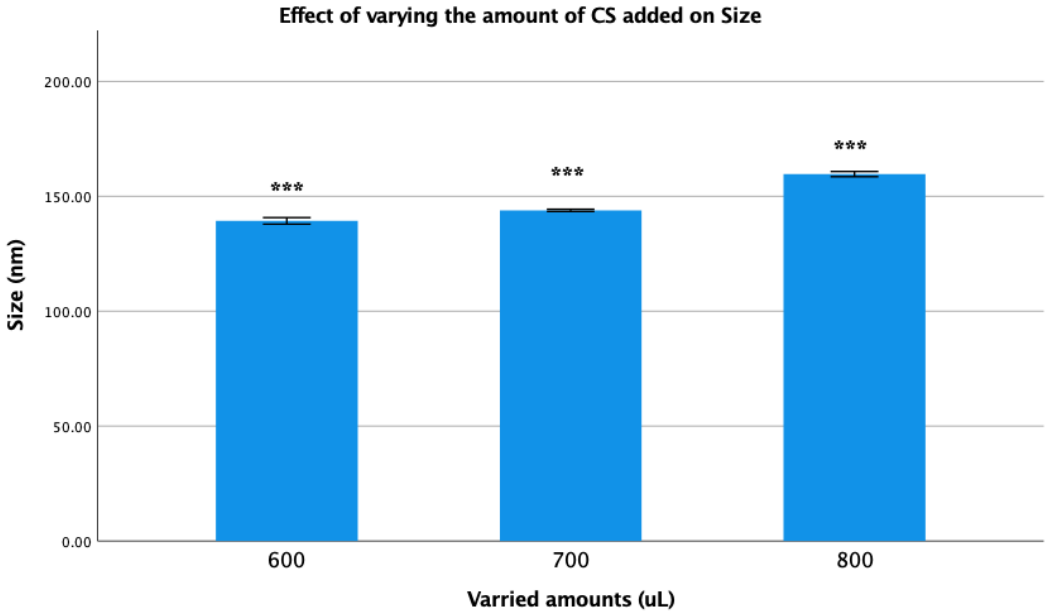

Figure 3.7 Effect of varying the amount of CS added on CCM-NPs on Size (nm) (*** P<0.001).

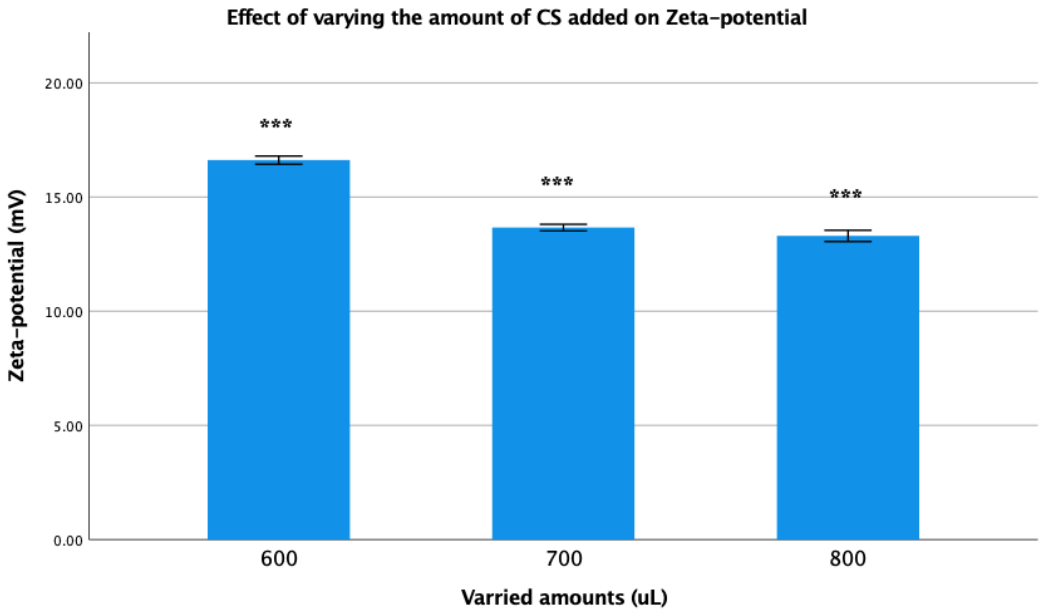

Figure 3.8 Effect of varying the amount of CS added on CCM-NPs on Zeta-potential (mV) (*** P<0.001).

Finally, the amount of curcumin (CUR) was varied (100, 200, 300, and 400 μL) on CCM-NPs, and Figures 3.9 and 3.10 expresses the size and zeta-potential of each formulation.

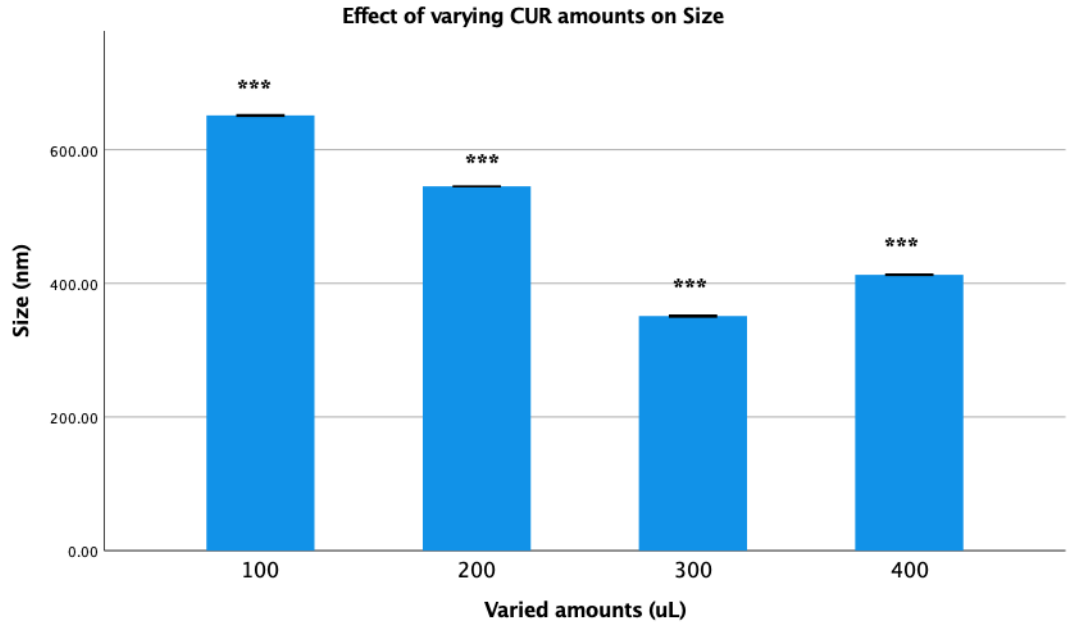

Figure 3.9 Effect of varying the amount of CUR added on CCM-NPs on Size (nm) (*** P<0.001).

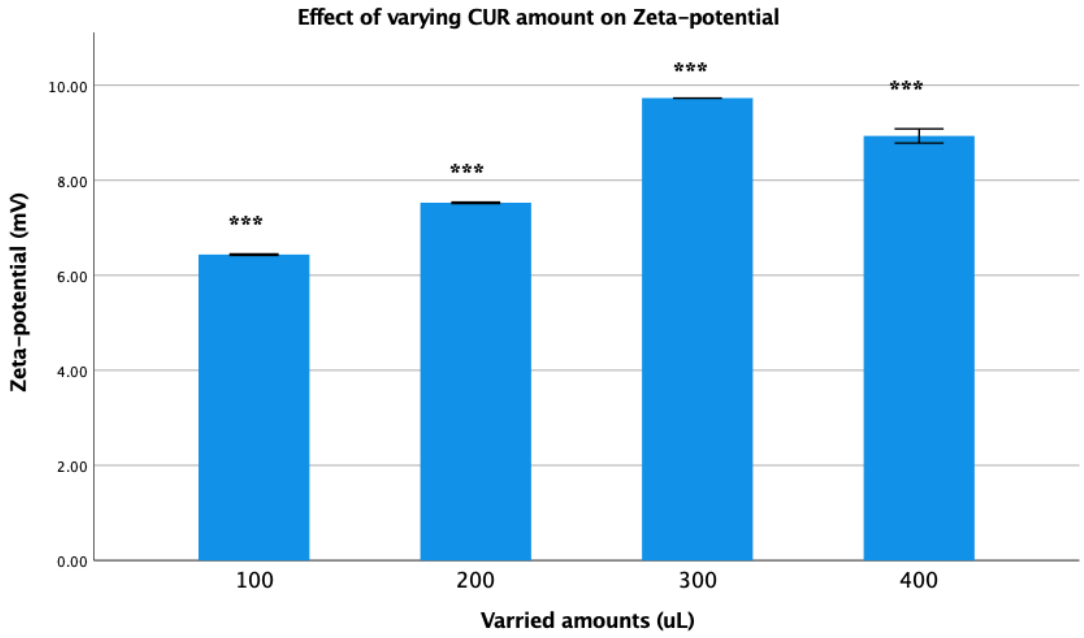

Figure 3.10 Effect of varying the amount of CUR added on CCM-NPs on Zeta-potential (mV) (*** P<0.001).

3.2 XRD

X-ray diffraction analysis was performed to study the crystallographic transformations, if any, of curcumin, chitosan, MCP1, CP, and CCM-NPs as shown in Figure 3.11.

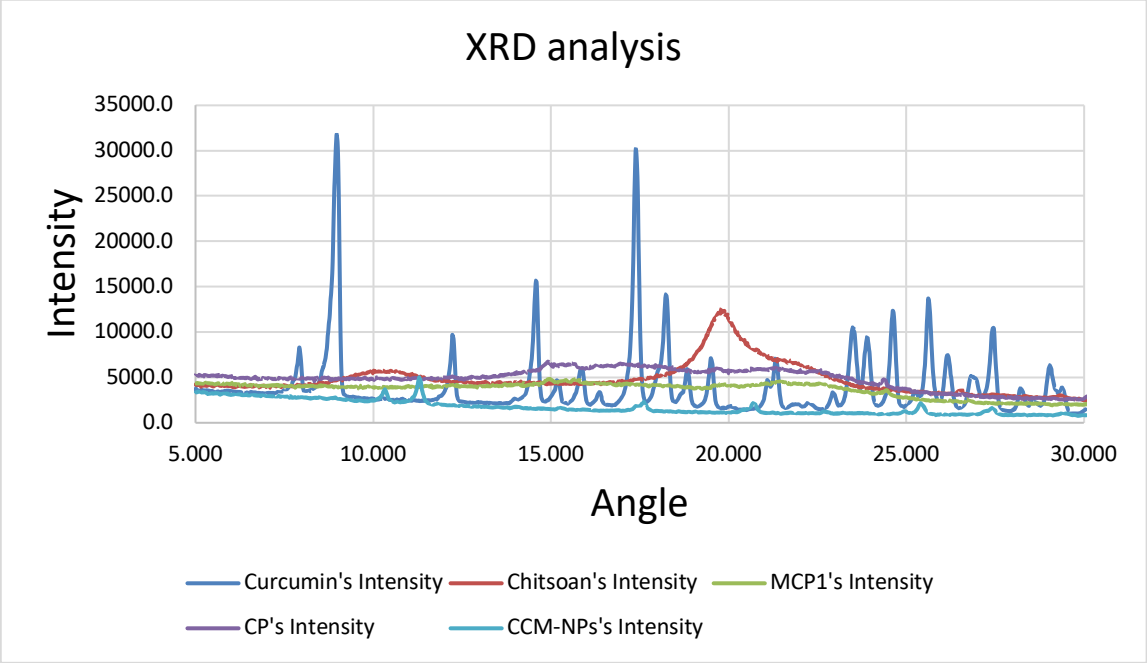

Figure 3.11 XRD analysis of free curcumin, chitosan, MCP1, CP, and CCM-NPs.

3.3 FT-IR

Fourier Transform Infrared Spectroscopy (FT-IR) was used to identify relevant functional groups in the formulations and raw materials. The spectra of CP, MCP1, MCP2, and MCP4 samples are shown in Figure 3.12, while the spectra of MCP1-NPs and CCM-NPs samples are presented in Figures 3.13.

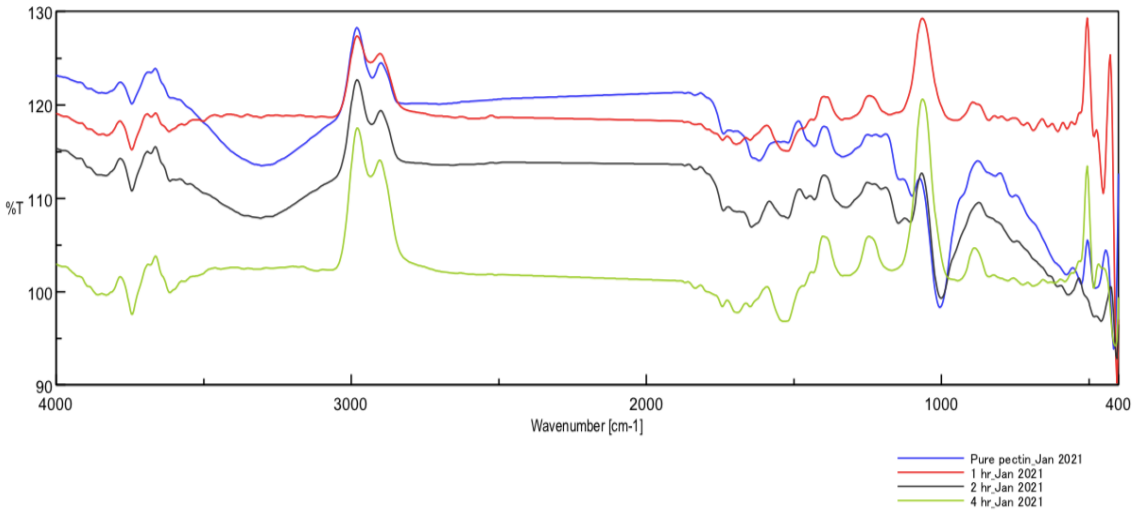

Figure 3.12 FT-IR spectroscopy of the natural pectin compared to the MCP samples of 1h, 2h and 4h.

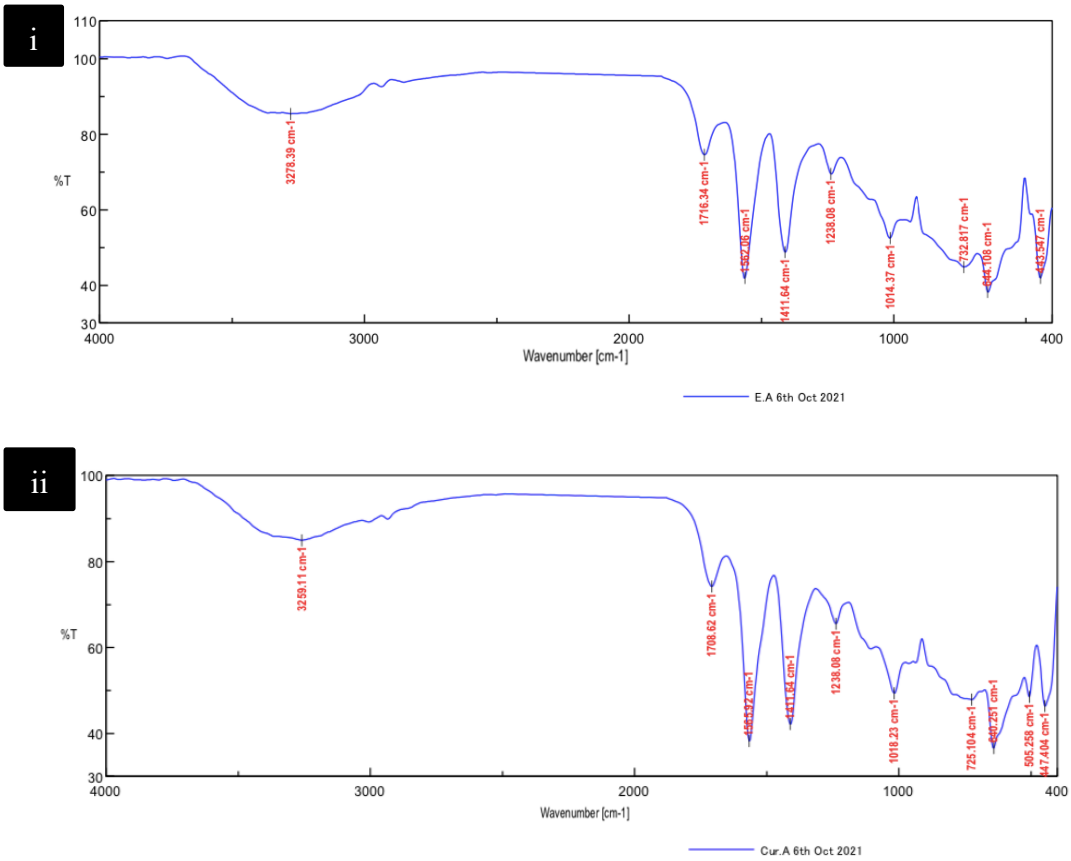

Figure 3.13 FT-IR spectroscopy of (i) MCP1-NPs, and (ii) CCMP-NPs.

3.4 SEM & AFM analyses

The SEM images of the prepared MCP-NPs and CCM-NPs are shown in Figure 3.14. The AFM was also used to observe and study the morphology of the prepared nanoparticles of MCP1-NPs, MCP2-NPs, MCP4-NPs, and CCM-NPs as shown in Figure 3.15.

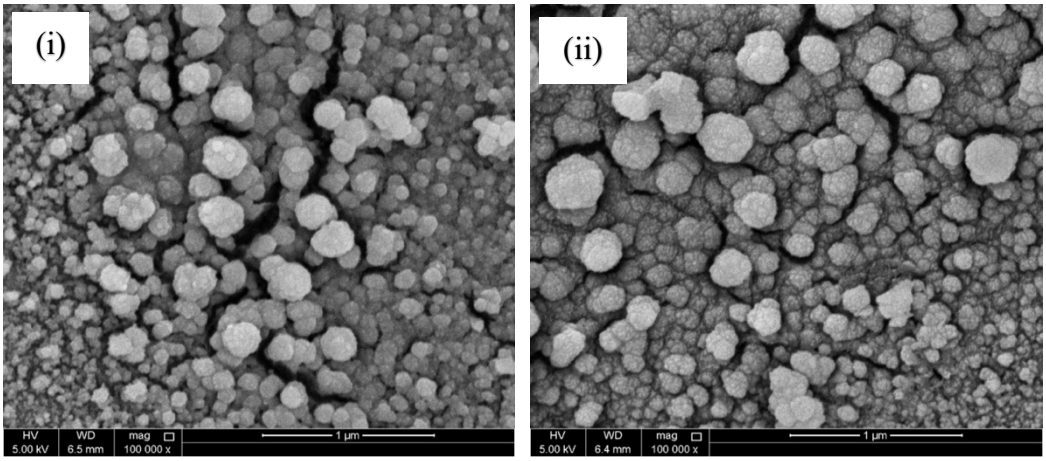

Figure 3.14: SEM images of MCP-NPs (i) and CCM-NPs (ii).

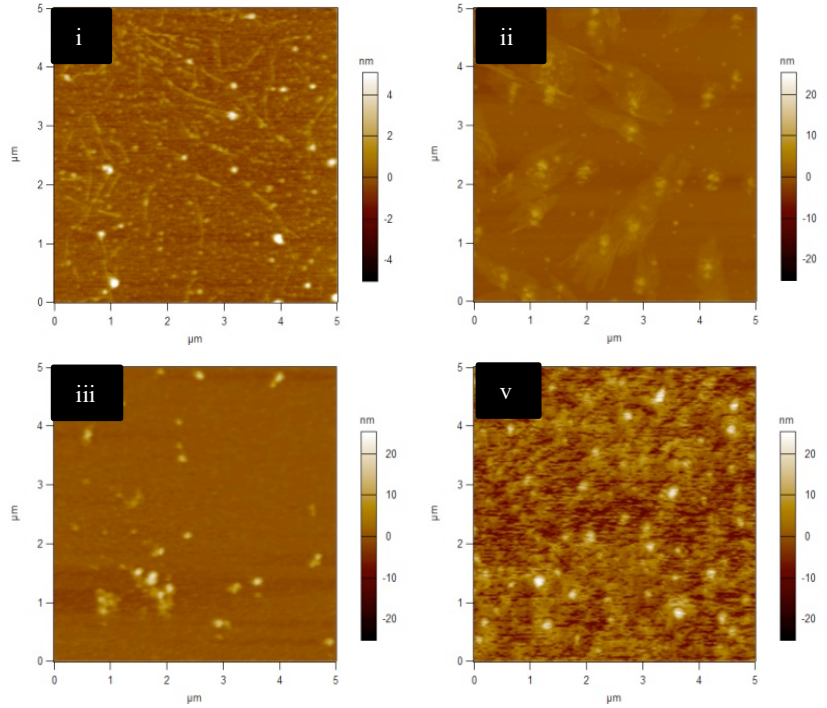

Figure 3.15 AFM scanning images of MCP1-NPs (i), MCP2-NPs (ii), MCP4-NPs (iii), and CCM-NPs (v).

3.5 TGA

The thermal stability of free curcumin, chitosan, MCP1, CP, CCM-NPs, and MCP-NPs were evaluated by thermogravimetric analysis (TGA), to determine the thermal changes of each as a function of temperatures. This is critical as it has a direct bearing to how they respond to relevant processing. Figure 3.16 shows the thermogravimetric analysis (TGA) of each sample.

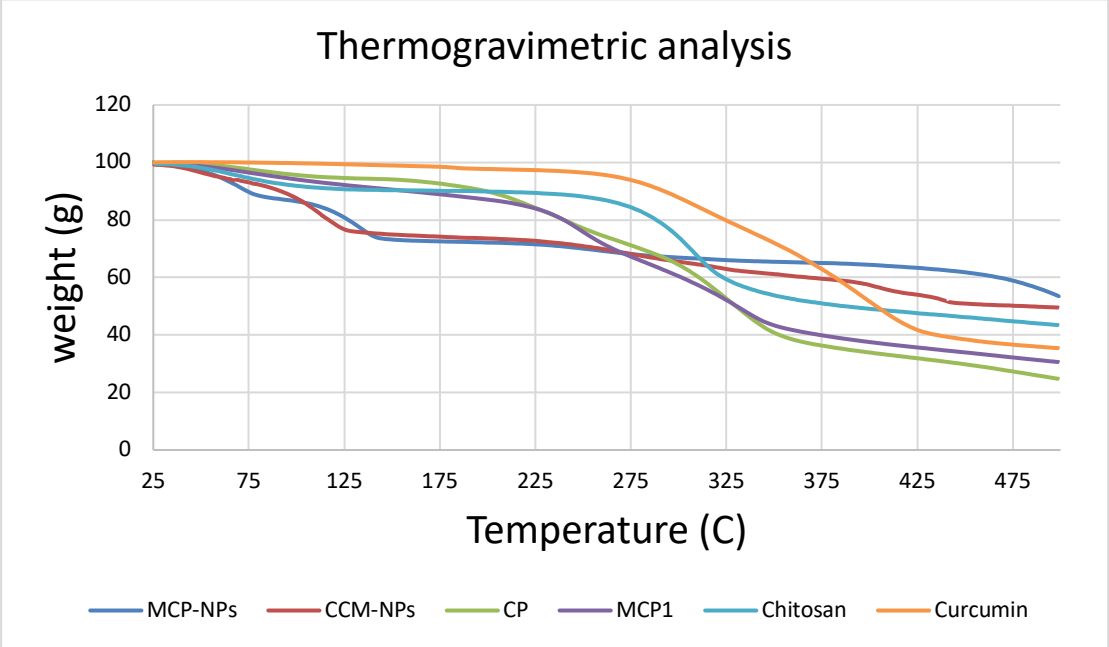

Figure 3.16 Thermogravimetric analysis of free curcumin, chitosan, MCP1, CP, CCM-NPs, and MCP-NPs.

3.6 Determination of encapsulation efficiency

To determine the encapsulation efficiency (EE%), a standard curve of curcumin was prepared in methanol (0.005, 0.01, 0.015, 0.02, and 0.03 mg/mL), which is used to quantify the curcumin concentration represented as peak areas in the chromatogram. The linearity of the standard curve is shown in Figure 3.17, with R^2 of 0.9816. The EE% was calculated using equation is 99.63%.

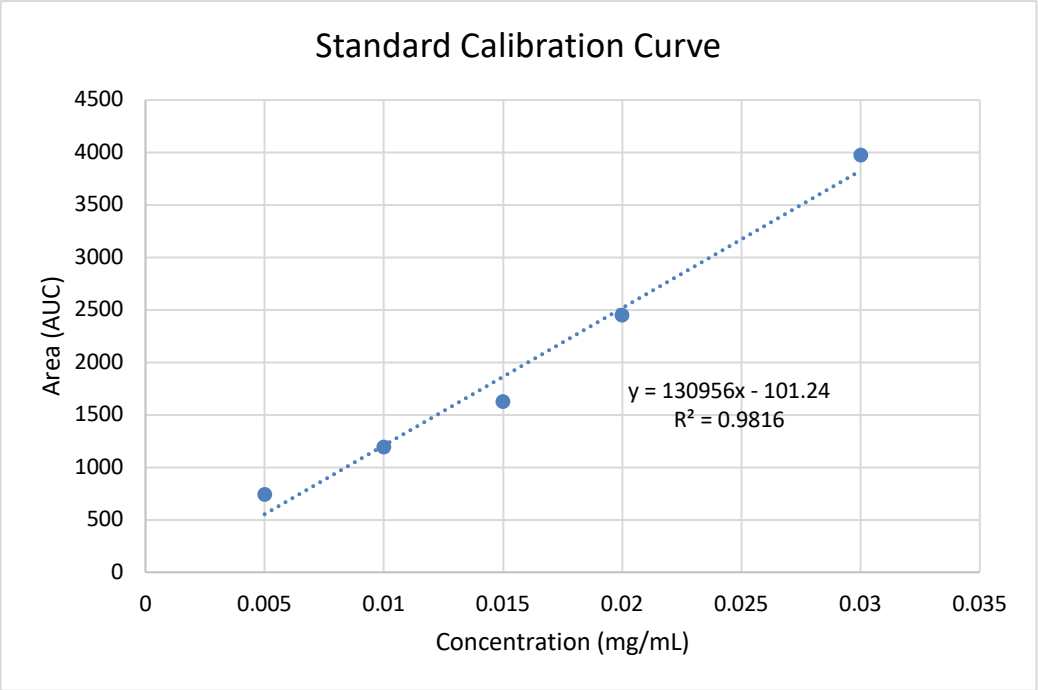

Figure 3.17 Standard calibration curve of curcumin.

3.7 Curcumin stability test as a function of exposure to light

Curcumin concentration from the stability studies in room light, sun light and in dark were conducted after exposing curcumin solutions to different time intervals of 0, 30, 60, 120, 240, and 360 minutes, followed by HPLC analysis. Figure 3.18 shows concentration of curcumin in different conditions as a function of time.

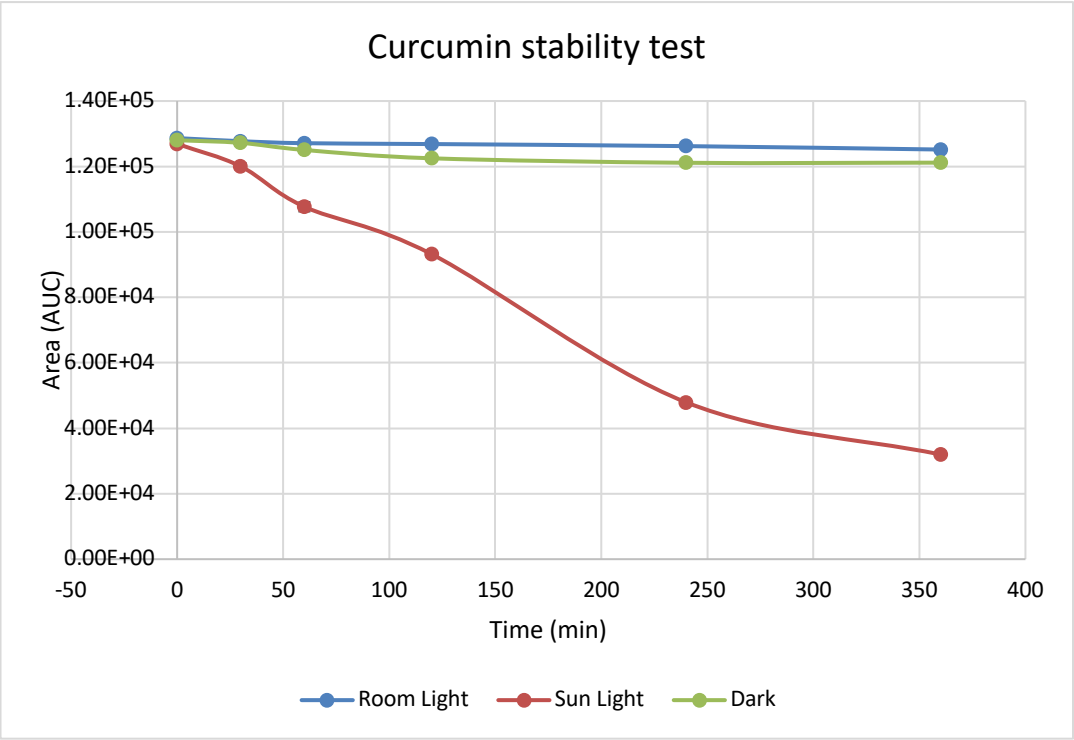

Figure 3.18 Curcumin stability test in room light, direct sun light, and in dark as a function of time.

3.8 Curcumin stability in the prepared NPs due after storage

The stability of curcumin in the prepared nanoparticles (CCM-NPs) were studied in two different storage conditions: 4°C and 37°C for (0, 1, 7, and 14 days). Physical parameters including size, zeta-potential, and PDI were determined and presented in Figures 3.19.

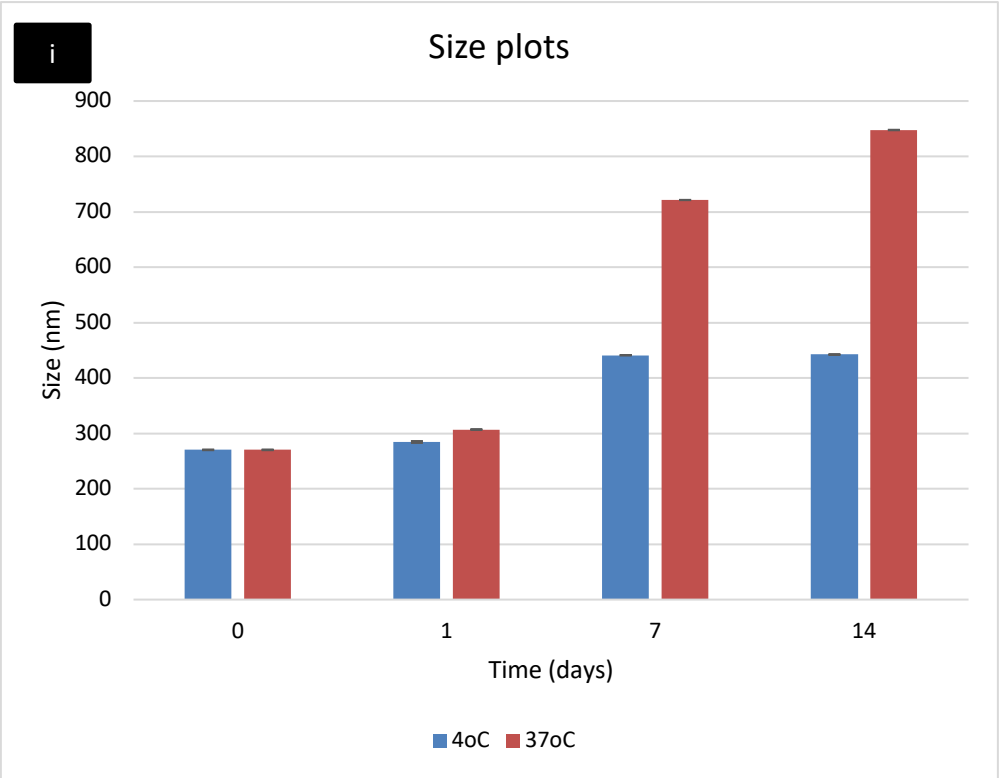
i
Size plots
900
800
700
600
500
400
300
200
100
0
Size (nm)
0
1
7
14
Time (days)
4oC
37oC

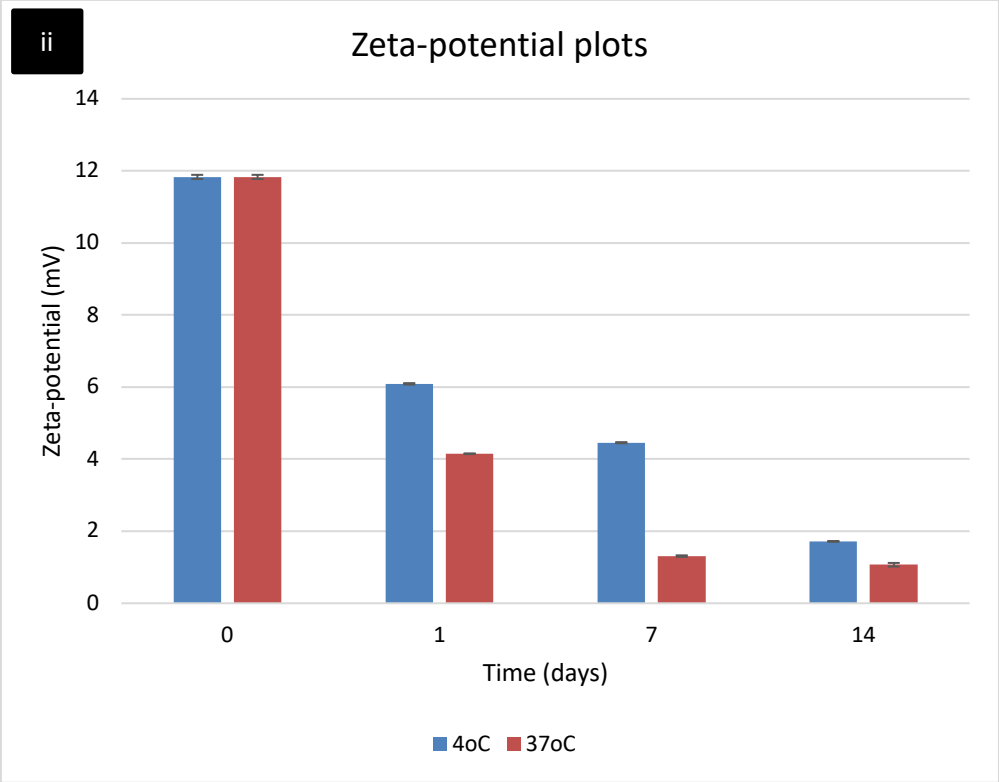
ii
Zeta-potential plots
14
12
10
8
6
4
2
0
Zeta-potential (mV)
0
1
7
14
Time (days)
4oC
37oC

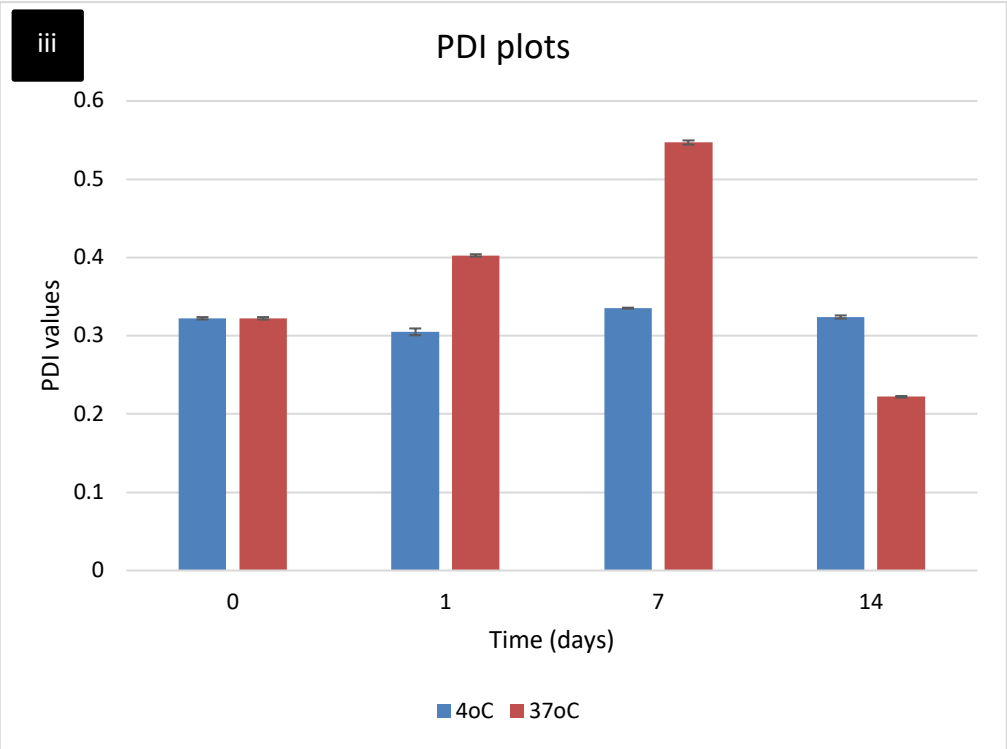

Figure 3.19 Size changes at 37oC and 4oC as a function of time (i), Zeta potential changes at 37oC and 4oC as a function of time (ii), and PDI changes at 37oC and 4oC as a function of time (iii).

3.9 Drug release

Curcumin release from CCM-NPs were studied over a period of 72 hours with aliquots taken from the sampling vials at 10-minute intervals. In Figure 3.10, the drug release at pH=6.8 for the time intervals (0, 1, 4, 6, 24, 48, and 72 hours) was observed.

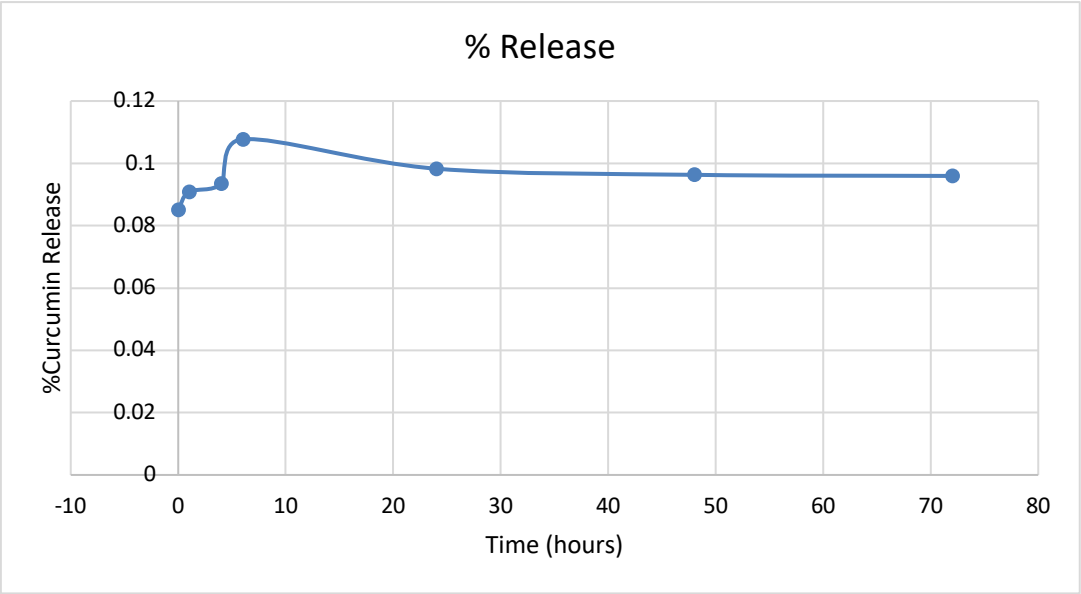

Figure 3.20 Drug release profile of CCM-NPs at pH=6.8 over a period of 72 hours.

3.10 Cell viability assay

Figures 3.21-3.23 shows the effect of varying the concentrations of free curcumin (2, 2.5, 5, 10, and 15 μg/mL) for 24, 48, and 72 hours, to determine the IC_{50} to be used in further cell viability studies using the formulated nanoparticles (CCM-NPs).

Figures 3.24-3.26 show the effect of varying the concentrations of MCP1, MCP2, and MCP4 (10, 20, and 40 μg/mL). Concentrations of the free curcumin and the prepared nanoparticles, shown in Figures 3.27 and 3.28, based on the calculated IC_{50} for 24, 48, and 72 hours, were studied to compare between the anticancer effect of free curcumin and CCM-NPs on cancer cell lines.

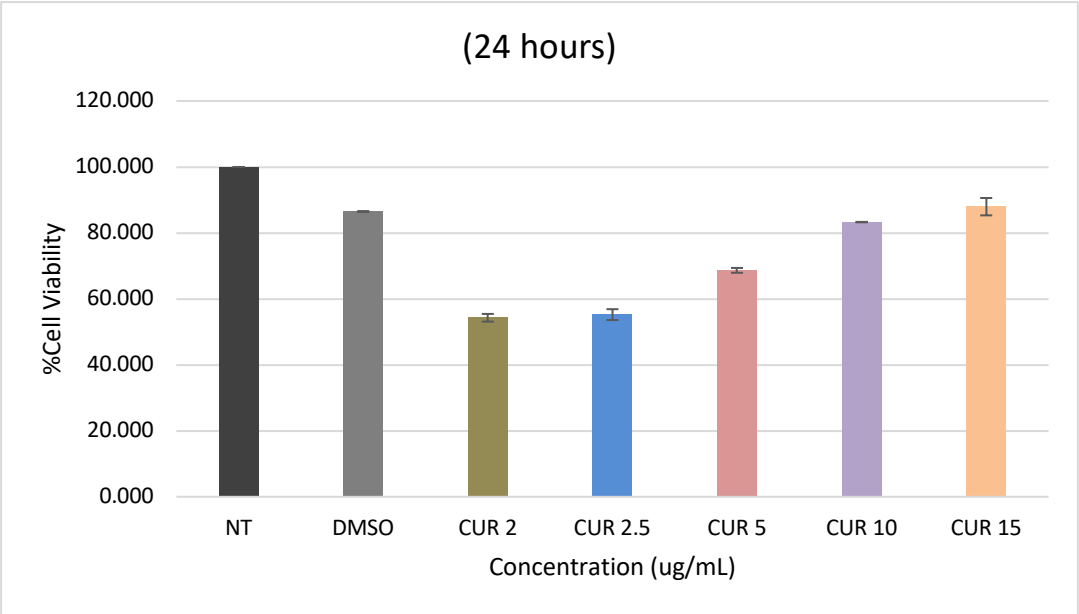

Figure 3.21 HCT-116 cell viability determination of free curcumin's IC50 after 24 hours.

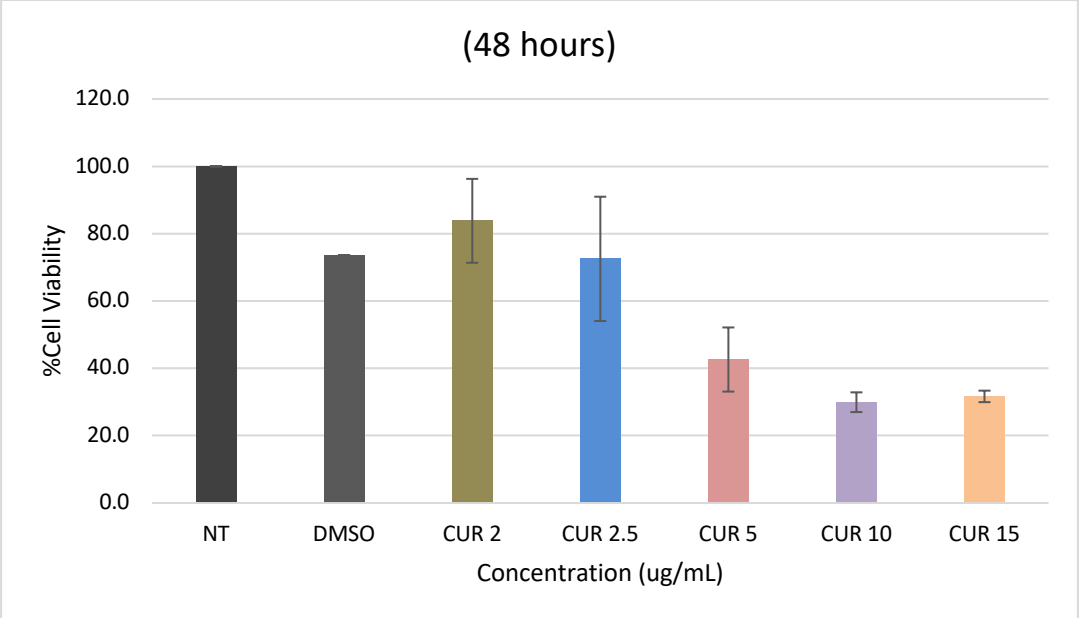

Figure 3.22 HCT-116 cell viability determination of free curcumin's IC50 after 48 hours.

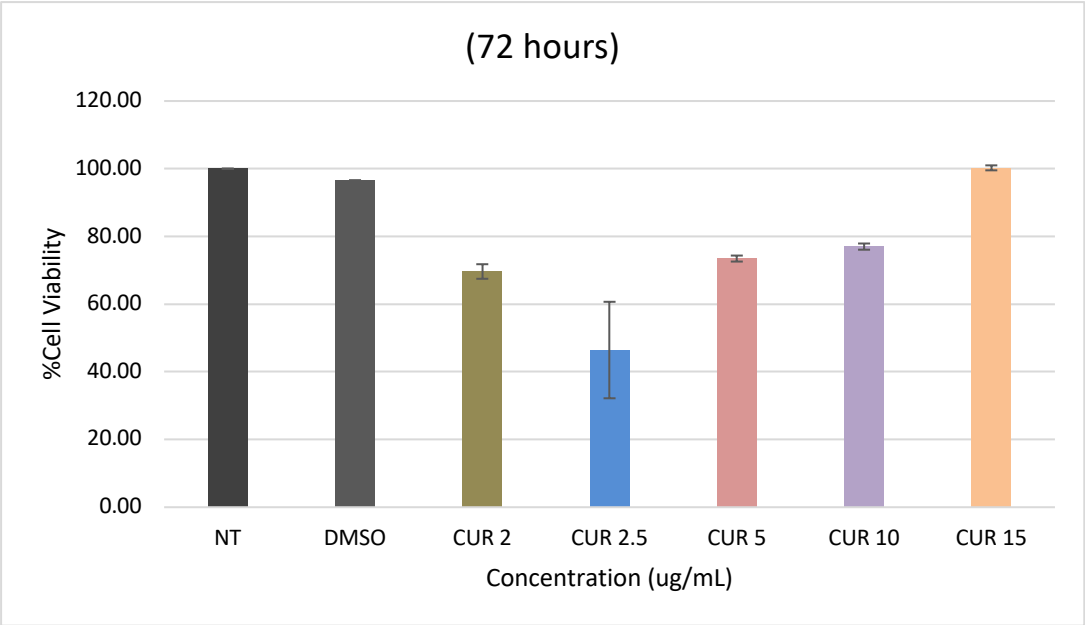

Figure 3.23 HCT-116 cell viability determination of free curcumin's IC50 after 72 hours.

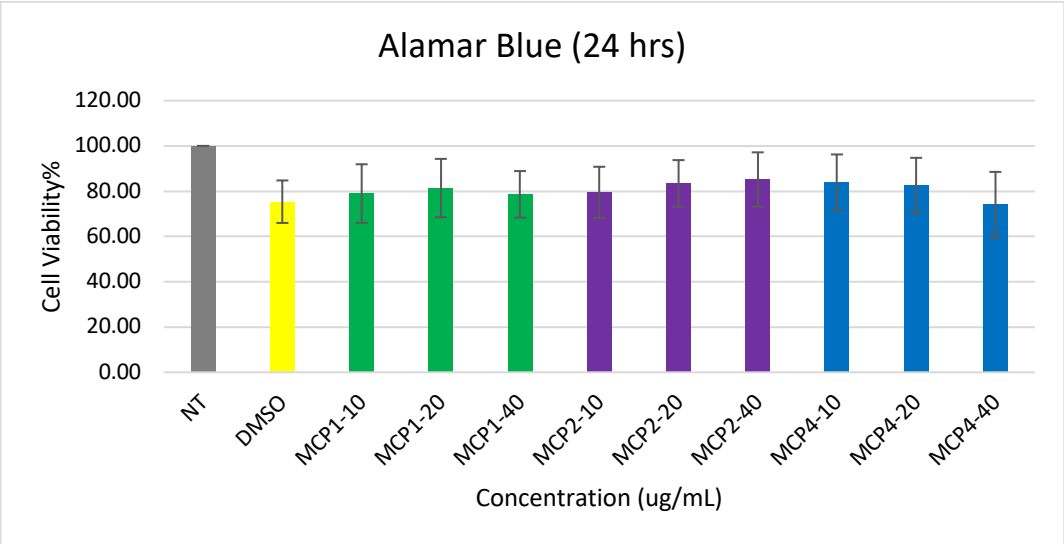

Figure 3.24 HCT-116 cell viability determination of MCP1, MCP2, and MCP4's IC50 after treatment for 24 hours.

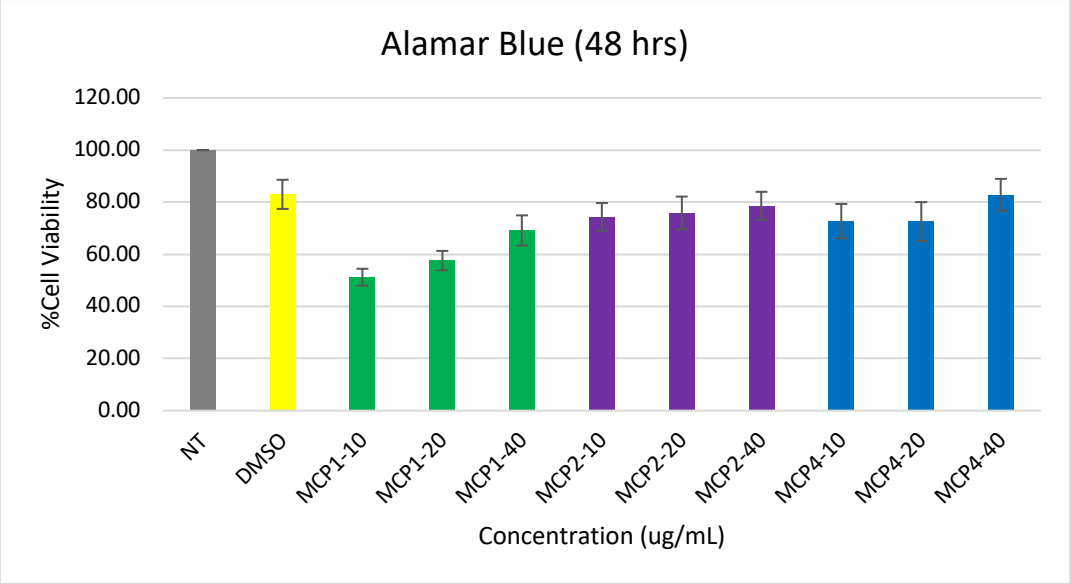

Figure 3.25 HCT-116 cell viability determination of MCP1, MCP2, and MCP4's IC50 after treatment for 48 hours.

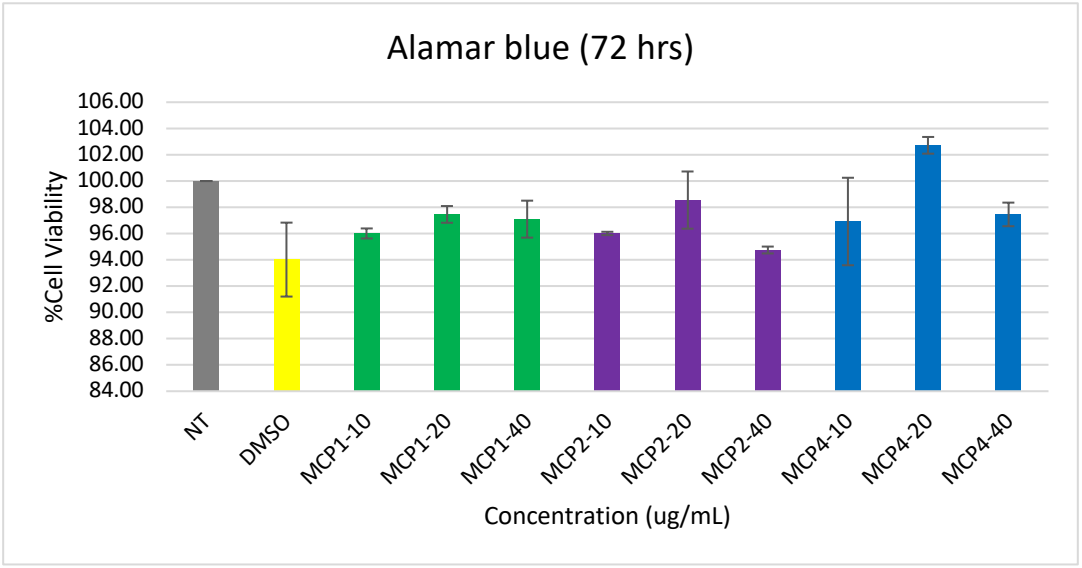

Figure 3.26 HCT-116 cell viability determination of MCP1, MCP2, and MCP4's IC50 after treatment for 72 hours.

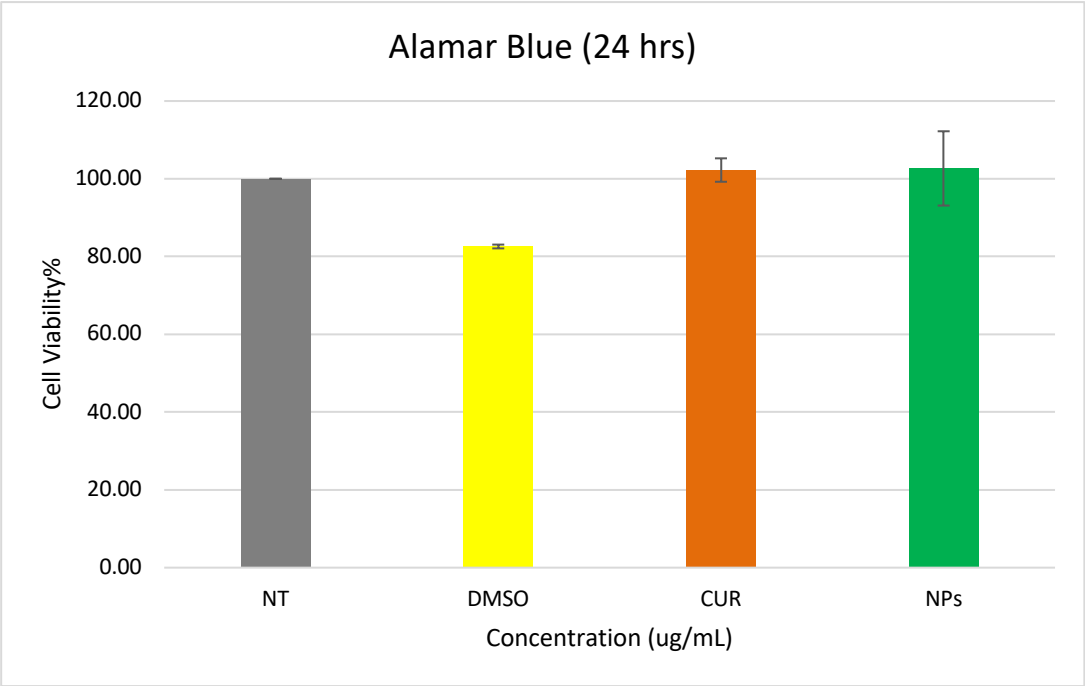

Figure 3.27 HCT-116 cell viability of free curcumin compared to CCM-NPs after treatment for 24 hours.

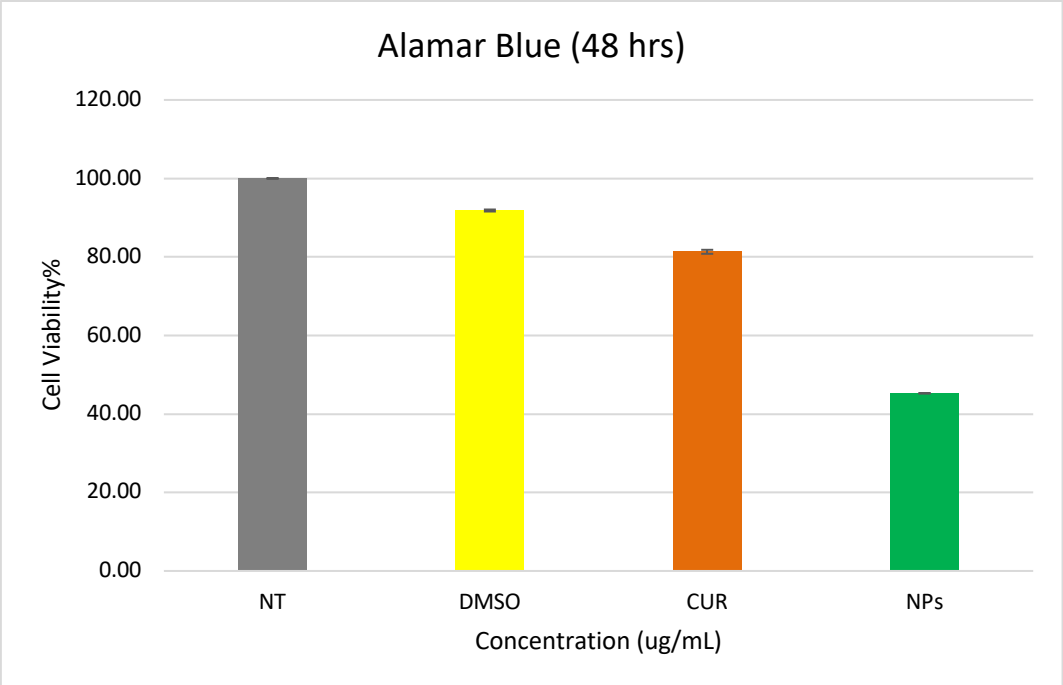

Figure 3.28 HCT-116 cell viability of free curcumin compared to CCM-NPs after treatment for 24 hours.

CHAPTER 4: DISCUSSION

Pectin polysaccharides consist of HG, RG-I and RG-II side chain polymers. The backbone of the HG is covalently cross-linked to the rhamnogalacturans, which contain branched arabinogalactan side chains (68). An alkaline treatment of pectin causes the side chains of rhamnogalacturan to be disrupted, resulting in the depolymerization of the backbone and the de-esterification of the HG regions (76). As a result of sustained exposure to alkaline pH, rhamnogalacturans are transformed into arabino galactans and galactans, which are crucial to the anticancer trigger cascade. Further, when CP was modified, the stirring effect was studied during the modification method. Three MCP samples were prepared, and named MCP1, MCP2, and MCP4. After modification, MCP was used to prepare MCP-NPs and CCM-NPs by ionic gelation as described previously. Subsequently, the chitosan polysaccharide was dissolved in an aqueous acidic solution which is 2% acetic acid to form the cations (positively charged). The prepared solution was added to MCP sample dropwise, followed by the addition of sodium tripolyphosphate (STPP) dropwise. The complexation between the opposite charged molecules, caused the formation of the spherical particles (65).

The introduction of MCP and chitosan as polymers enhances the nano-mechanical formulation's strength and hydrophobicity, which is anticipated to reduce the rate and amount of drug release from the nanoparticle to the surrounding dissolution media (69). Furthermore, to determine the optimum conditions necessary for formulation a series of formulations were studied and the results were shown in figures 3.1-3.10 in chapter 3. In figures 3.1 and 3.1, the effect of varying STPP concentration of MCP-NPs formulations was studied. An increase in STPP concentration from 0.5 mg/mL to 1 mg/mL produced larger sized nanoparticles and the zeta potential was reduced accordingly. In figures 3.3 and 3.4, the effect of varying CS concentration of

MCP-NPs formulations showed that an increase in concentration of chitosan from 0.5 mg/mL to 1 mg/mL produced larger sized nanoparticles and the zeta potential was reduced. When CS concentration increases, more of the protonated amino groups of chitosan molecules become accessible to coacervate with MCP and cross-link with STPP, which is manifested in increase of size from 173.6 nm to 229.2 nm for the CS-MCP1 samples as an example. Among the three prepared formulations (MCP1-NPs, MCP2-NPs, and MCP4-NPs), MCP1-NPs produced the smaller sample sizes and the best zeta-potential values while determining the optimum conditions in all variations. Thus, MCP1 was used for further analysis, characterizations, and in preparing CCM-NPs.

Further, the variation of STPP, CS, and CUR amounts were studied to determine the optimum conditions to prepare CCM-NPs and the results were shown in figures 3.5-3.10. In figure 3.5, the effect of varying the amount of STPP to on the CCM-NPs was studied and shows that increasing the amount of STPP produced larger nanoparticles. There was a slight increase in the size of the nanoparticles, from 209.4 $\pm$ 0.30 nm in 1AC to 257.5 $\pm$ 0.62 nm in 1CC having the highest amount of STPP, but the difference in zeta potential was noticed to be reduced while increasing the amount of STTP, from 10.6 $\pm$ 0.02 mV to 5.22 $\pm$ 0.01 mV (Appendix C). Furthermore, in figure 3.6, the effect of varying the amount of CS showed that increasing the amount of CS produced larger nanoparticles. The size ranged from 139.3 $\pm$ 0.57 nm in 2AC to 159.7 $\pm$ 0.46 nm in 2CC with the highest amount of CS. The difference in zeta potential was noticed to be reduced while increasing the amount of CS, from 16.6 $\pm$ 0.07 mV in 2AC to 13.3 $\pm$ 0.10 mV in 2CC (Appendix D). Finally, in figures 3.9 and 3.10, the effect of varying CUR showed that increasing the amount of CUR produced smaller nanoparticles. The reduction in size of the nanoparticles was from 651.3 $\pm$ 0.40 nm in 3AC to 412.9 $\pm$

0.31 nm in 3DC having the highest amount of CUR, and the difference in zeta potential was noticed to be increased while increasing the amount of CUR, from 6.44 $\pm$ 0.006 mV in 3AC to 8.93 $\pm$ 0.06 mV in 3DC (Appendix E). This increase in the surface charge is directly related to the increase in size, whereby, bulkier particles hinder the knitting effects of STPP with the free amino groups of chitosan. This leaves relatively more of the free amino group in the nanoparticle matrix, with a consequent increase in zeta potential. However, 3CC had the best size and zeta-potential, hence, the best amount of CUR to be added while preparing the nanoparticles is 300 μL. With the incorporation of curcumin, the attributable to the stearic effects by curcumin within the polymer chain domains during coacervation between MCP and chitosan, impedes the process.

X-ray diffraction (XRD) is commonly used to study the crystalline structure of materials. This technique measures the average spacing between the layers or rows of atoms/molecules (70). The XRD analyses of free curcumin, chitosan, MCP1, CP, and CCM-NPs are shown in figure 3.12 in chapter 3. The diffractogram of curcumin shows multiple peaks between 5^{o} and 30° which were mainly attributed to its crystalline nature. These distinctive peaks were disappeared in the CCM-NPs, implying that curcumin's crystalline constitution had given way to an amorphous state. This change in physical properties might be caused by molecular interactions between curcumin and chitosan during formulation (71). However, the diffractogram of chitosan, MCP1, and CP shows an amorphous state.

An FT-IR was made for CP, MCP1, MCP2, MCP4, MCP1-NPs, and CCM-NPs (Figures 3.13) to make sure that the desired compound is formed and to study the influence of stirring effect when modifying CP. In CP, the wide peak at approximately 3301 cm^{-1} represents the secondary hydroxyl carboxylic groups, but in comparison to

MCP1, the peak is not shown; this could be due to the methyl esterification of the carboxylic groups along the pectin backbone (72). In addition, the C-H stretching of the carbohydrate unit was found at approximately 2935 cm^{-1}, and the -C=O stretch was found at approximately 1697 cm^{-1}, and finally, the -C-O stretches was found at 1338 cm^{-1}. In the MCPs spectrum, a distinct absorption band are observed at 1015 cm^{-1}, while it is not apparent in the CP spectrum, which is consistent with an increase in D-galacturonic acid sugar units, thus confirming that the modification yielded the desired galactan moiety. In figure 3.3 of chapter 3, the FT-IR of MCP1-NPs and CCM-NPs are shown. The major peaks of raw materials were disappeared in the prepared MCP1-NPs and CCM-NPs. For example, the amine group of chitosan which shows at approximately 1650.68 cm^{-1}, the phosphate group peak of STTP which shows approximately at 1211.47 cm^{-1} and the D-galacturonic acid peak of MCP which shows approximately at 1015.02 cm^{-1}; this can be due to the crosslinking effect of chitosan with MCP, curcumin and STPP. The relatively sharper peaks at 3278.39 cm^{-1} and 3259.11 cm^{-1} in the spectra of the MCP1-NPs and CCM-NPs, respectively, represents a higher density of hydroxyl (-OH) moieties. The intense peaks at 1562.06 cm^{-1} and 1565.92 cm^{-1} in both spectra (MCP-NPs and CCM-NPs) presents the shifted peaks of amine in the raw materials from the 1600–1700 cm^{-1} region. This represents the deformation of the NH caused by the interaction between the carboxylic groups of MCP and the amino groups of chitosan. The only difference observed between the MCP-NPs and the CCM-NPs spectrums is the peak at 1411.64 cm^{-1}, indicating the presence of curcumin in the formulation.

The morphology of the MCP-NPs and CCM-NPs were observed using SEM and AFM and the results are shown in Figures 3.14 and 3.15 in chapter 3. The picture indicated evenly dispersed and spherically shaped nanoparticles, which corresponded

to the size measurements made by DLS research.

A thermogravimetric analysis is important to determine the temperature at which compounds will change and the limit temperatures at which they can be used without losing their properties. Thus, thermogravimetric analysis (TGA), which measures mass change as a function of temperature, was used to evaluate the thermal stability of MCP-NPs, CCM-NPs, and the raw materials (CP, MCP1, Chitosan and Curcumin) (Figure 3.16). The weight loss of chitosan occurred in two temperature ranges, being the first one from 67ºC to 225ºC and the second from 275°C to 319 °C; this is associated with loss of mass which is related to moisture loss (6% loss of mass) and thermal degradation (33% loss of mass). Further, the loss for curcumin was 56% occurring from 260°C to 441°C; this occurs during the decomposition of the curcumin substituting group followed by the benzene rings (73). Moreover, the weight loss of CP and MCP1 occurred in two temperature ranges, the first one from 182°C to 290°C for CP and from 100°C to 198°C for MCP1, the second from 296°C to 380°C for CP and from 224°C to 380°C for MCP1; this behavior is associated with the moisture loss (25% of CP and 7% of MCP1 loss of mass) and the thermal degradation (30% of CP and 45% of MCP1 loss of mass), thus confirming that the modification of CP yielded with better thermal stability that the one for CP only. The thermal stabilities of MCP-NPs and CCM-NPs occurred in three temperature ranges, the first one from 66°C to 77°C for MCP-NPs and from 48°C to 77°C for CCM-NPs, the second being from 108°C to 173°C for MCP-NPs and from 107°C to 138°C for CCM-NPs, the third being from 224°C to 351°C for MCP-NPs and from 378°C to 439°C for CCM-NPs; this behavior is associated with the moisture loss (4% of MCP-NPs and 5% of CCM-NPs loss of mass), the decomposition degradation (9% of MCP-NPs and 9% of CCM-NPs), and the

thermal degradation (8% of MCP-NPs and 7% of CCM-NPs loss of mass); the higher thermal stability of CCM-NPs could be associated with the interaction between NP and curcumin, whose phenolic compounds show great thermostability (73). The coating barrier formed by chitosan showed its effectiveness toward preserving the integrity of the structure and in maintaining the high thermal stability of curcumin.

Encapsulation is the use of technologies to entrap an active agent within a material system that may release its payload at regulated rates under certain conditions (74). This procedure guarantees regulated release and protects labile chemicals from severe environmental conditions. Two important factors of nanomedicines are encapsulation efficiency and drug loading. They are both primarily determined by the amount of medicine in the feed, the manufacturing process used, the physicochemical properties of the component polymers (such as their hydrophilicity/hydrophobicity and solubility), and other experimental circumstances (75,76). The encapsulation efficiency of CCM-NPs was 99.63%. This rise is most likely owing to the modified citrus pectin's decreased molecular weight, which is induced by the elimination of neutral sugars during the modification process (77). Usually, when z-potential increases with molecular weight, shorter chains have more carboxylic acid end groups (78) to react with chitosan, hence, it allows more curcumin to diffuse and encapsulate within the chitosan-MCP matrix. Furthermore, the encapsulation efficiency reported in this work is greater than that found in a number of previous studies that used a pectin-chitosan matrix for drug encapsulation. For example, Hwang S.W. and Shin J. W. found a curcumin-loaded chitosan-pectin microparticle encapsulation efficiency of 62.9% (79). In another work, Maciel et al. reported an encapsulation efficiency of 62 % using a polyelectrolyte complex system of chitosan-pectin nano-and microparticles to encapsulate the hormone insulin (80).

Curcumin stability test was made to test the degradation levels of curcumin toward different light conditions (room light, sun light, and in dark). According to Figure 3.18 in chapter 3, it was shown that curcumin degrades the fastest in sun light, as it shows the highest rate of degradation compared to the room light and in dark conditions of light. Thus, curcumin must be stored in amber colored bottles to prevent its photo oxidation and degradation (89,90).

The storage stability of a drug in a dosage form is important since it determines the likely life span of that specific formulation (81). This experiment was conducted to study the impact of storage, in a cold temperature (4^{o}C), on the physical properties of CCM-NPs. Figure 3.19 shows the changes in size (i), zeta-potential (ii), and PDI (iii) over 14 days period. Figure 3.19 (i) shows a gradual increase in size of CCM-NPs over 14 days (from 270.3 ± 0.636 to 442.4 ± 0.503 nm). However, when CCM-NPs were stored in 37^{o}C, the size has significantly increased from 270.3 ± 0.636 nm to 847.7 ± 0.451nm over the 14 days. Further, in Figure 3.19 (ii), the zeta-potentials of CCM-NPs that were stored at 4^{o}C, were gradually decreasing over the 14 days (from 11.83 ± 0.057 mV to 1.72 ± 0.011 mV), however, for CCM-NPs that are stored at 37^{o}C decreased significantly over the 14 days (from 11.76 ± 0.055 mV to 1.07 ± 0.05 mV). This is due to Ostwald's ripening, which occurs when smaller particles with a high surface area to volume ratio agglomerate and deposit on bigger particles in order to decrease their surface energy (81). Also, it was noticed in Figure 3.19 (iii) that the PDI of CCM-NPs stored at both 4^{o}C and 37^{o}C over the 14 days was lower than 0.5 but increased only once to 0.547 ± 0.002 after 7 days of storage in 37^{o}C. Typically, the particle size influences the degradation of polymeric nanoparticles, and bigger particles are thought to contribute to quicker polymer breakdown (82). This is because the polymer matrix of large particles increases the period of release owing to the longer distance and may

also result in autocatalytic degradation of the polymer substance (83). These findings indicate the low storage stability of CCM-NP, hence, the NPs should be utilized within two weeks of production or stored as dry and reconstituted before use.

Drug release profiles of the CCM-NPs were studied over a period of 72 hours. In Figure 3.20, a slight release was observed in the formulation, followed by a slower release and eventually a plateau over the period of 72 hours. Drug release was faster within the first 6 hours compared to the rest of duration. However, the drug release in this experiment is considered very low in comparison to previous studies. For example, in a study done by Lay Hong et al., the drug release profiles were between 50% to 80.5 over a period of 6 hours (84).

Curcumin's limited bioavailability and solubility are important constraints in its usage as an effective anticancer treatment. A targeted nano-formulation of curcumin, on the other hand, serves to increase its bioavailability and deliver greater cytotoxic effects against cancer cells at the site of action (85). Two different determinations of IC_{50} experiments were made. Firstly, in order to determine the IC50 of free curcumin, variable concentrations of free curcumin (2, 2.5, 5, 10, and 15 μg/mL) were prepared as treatments and were tested for 24, 48, and 72 hours on HCT-116 cell lines. In Figures 3.21-3.23, the cell viability plot reveled an overall decrease in cell viability when the treatment concentration increased over the 72 hours period, showing a dose- and time-dependent manner. The determined IC_{50s} of free curcumin at each time point are: 8.5 μg/mL at 24 hours, 5 μg/mL at 48 hours, and 2.5 μg/mL at 72 hours. In Figures 3.24-2.26, the determination of MCP1, MCP2, and MCP4 IC_{50s} were studied over a variable concentration of (10, 20, and 40 μg/mL) at 24, 48, and 72 hours. After 48 hours of treatment, MCP formulations showed a decrease in cell viability when the concentration of the treatment increased. This is due to the anticancer effect of MCP

and the influence of galectin yield on MCP that enhances the anti-cancer properties of MCP (49). The determined IC_{50s} of each formulation were 34 μg/mL for MCP, and 39 μg/mL for MCP2. Lastly, in Figures 3.27 and 3.28, CCM-NPs reduced 54.74% $\pm$ 0.01% of cancer cells in comparison to free curcumin which reduced 18.69% $\pm$ 0.51% of cancer cells at a period of 48 hours. The greater cytotoxicity of CCM-NPs over free curcumin may be attributable to the fact that the citrus pectin modification process resulted in the formation of neutral sugar sequences with a low degree of branching but high galactose content. Galactose, as a powerful antagonist to Gal-3, can limit the proliferation and migration of colon cancer cells (96–98). As a consequence, the alamar blue assay findings demonstrate the formulation's safety against normal cells.

CHAPTER 5: CONCLUSION AND FUTURE WORK

5.1 Conclusion

Cancer is still one of the major causes of death globally. Despite its significant influence, oncology has one of the worst track records for experimental medications in clinical development. Its success rates are said to be more than three times lower than those of cardiovascular disease (54). The primary problems in cancer drug discovery are drug target selection, tumor biology variety, regulatory environment, and cost, all of which have led to barriers in cancer medication development (54,99). Natural products have been used as a source of treatments to heal human problems since the birth of medicine. Indeed, medications originating from natural sources continue to make significant contributions to drug discovery today, particularly in cancer treatment and chemoprevention (98,99). Further, Vincristine, etoposide, paclitaxel, flavopiridol, camtothecin, and homoharringtonine are plant-derived anticancer medicines that are now in clinical trials (98). However, the formulations of these anticancer medicines are frequently quite hazardous. For example, paclitaxel (Taxol®) is emulsified in Cremophor and dehydrated ethanol, which frequently causes severe and deadly hypersensitivity responses (100).

The goal of this research is to create a curcumin-encapsulated chitosan-nanoparticles drug delivery system for the possible treatment of colorectal cancer. It is anticipated that by utilizing non-toxic raw components in the formulation, this prospective therapeutic option will be non-toxic.

CCM-NPs were successfully prepared utilizing the simple ionic gelation process. The optimized formulation has a mean size of 270.3 nm ($\pm$0.636 nm) and a zeta potential of about +11.83 mV ± 0.057. The size of the NPs was appropriate for delivery to colon, and the zeta potential showed a stable system with no agglomeration. The

SEM pictures revealed the production of spherical NP with diameters consistent with the results of dynamic light scattering. Curcumin may interact with CS and STPP in CCM-NPs, according to FT-IR research. The curcumin EE% percent was determined to be at 99.63%, with a low curcumin release at the end of a 72-hour period.

The *in vitro* cytotoxicity studies showed the greater cytotoxicity of CCM-NPs over free curcumin, were CCM-NPs reduced 54.74% $\pm$ 0.01% of cancer cells in comparison to free curcumin which reduced 18.69% $\pm$ 0.51% of cancer cells at a period of 48 hours. The anticancer properties of MCP formulations were studied and showed their effectiveness in reducing the viability of cancer cells over a period of 72 hours.

To sum up, the current trend in drug delivery is toward the development of nanocarrier drug delivery systems, which are likely to have a significant influence on cancer therapy. Cancer therapy can be improved by intelligently constructing nanocarriers to suit the target of medication delivery. In this work, the effective production of CCM-NPs resulted in a considerable advantage in curcumin therapeutic efficacy when compared to free curcumin. The lack of visible toxicities and side effects connected with the therapy enhanced the promise of this delivery strategy. As a result, this provides proof-of-principle that incorporating curcumin into CCM-NPs might be a viable future therapy for colorectal cancer.

5.2 Suggestions for future work

Nanotechnology advancements have resulted in the development of several unique and successful medication compositions in cancer therapies. However, substantial study is required before a novel formulation may enter the clinical stage. A few proposals for future work are given below as an extension of the existing work.

Research can be conducted to improve the zeta-potentials of the current created nanoparticles. For example, using a low molecular weight chitosan may reduce the size of the nanoparticles slightly but may result in a better zeta-potential values of the created formulations.

Another research can conduct a better drug release profile. The inclusion of a surfactant in a delivery system may aid in providing a more regulated release profile over time.

Beside improving the zeta-potential and drug release profile, the current prepared nanoparticles can be tested on other cell lines, as in this current work, the nanoparticles cytotoxicity was only tested on HCT-116 cell lines. Examples of other common colorectal cancer cell lines are HT-29, SW480, Caco-2, LoVo, etc. In addition, other *in vitro* tests can be applied, such as cellular uptake, apoptotic assay, western blot, etc.

Finally, an *in vivo* monitoring of the prepared nanoparticles is an important target to check to the tumor response to the treatment with changes of the animal model used.

REFERENCES

1. Samuels A, Ward E, Feuer EJ, Thun MJ. Cancer Statistics , 2004. 2004;
2. Hamad Medical Corporation. Colorectal Cancer is Third Most Commonly Diagnosed Cancer in Qatar and a Leading Cause of Cancer-Related Deaths in the Country. 2018.
3. Cao J, Yang J, Wang Z, Lu M, Yue K. Modified citrus pectins by UV/H2O2 oxidation at acidic and basic conditions: Structures and in vitro anti-inflammatory, anti-proliferative activities. Carbohydrate Polymers. 2020;247(July).
4. Ridley BL, O'Neill MA, Mohnen D. Pectins: Structure, biosynthesis, and oligogalacturonide-related signaling. Vol. 57, Phytochemistry. 2001. 929–967 p.
5. Leclere L, Cutsem P Van, Michiels C, Zhang W, Xu P, Zhang H. Anti-cancer activities of pH- or heat-modified pectin. Trends in Food Science and Technology. 2013;4 OCT(2):1–8.
6. Meerasri J, Sothornvit R. Characterization of bioactive film from pectin incorporated with gamma-aminobutyric acid. International Journal of Biological Macromolecules. 2020;147:1285–93.
7. Yavarpour-Bali H, Pirzadeh M, Ghasemi-Kasman M. Curcumin-loaded nanoparticles: A novel therapeutic strategy in treatment of central nervous system disorders. International Journal of Nanomedicine. 2019;14:4449–60.
8. Mbese Z, Khwaza V, Aderibigbe BA. Curcumin and Its Derivatives as Potential Therapeutic Agents in Prostate, Colon and Breast Cancers. Molecules (Basel, Switzerland). 2019;24(23).
9. Sabra R, Billa N, Roberts CJ. Cetuximab-conjugated chitosan-pectinate

(modified) composite nanoparticles for targeting colon cancer. International Journal of Pharmaceutics. 2019;572(September):118775.

10. Sarika PR, James NR, Nishna N, Anil Kumar PR, Raj DK. Galactosylated pullulan-curcumin conjugate micelles for site specific anticancer activity to hepatocarcinoma cells. Colloids and Surfaces B: Biointerfaces. 2015 Sep 1;133:347–55.
11. Ding L, Ma S, Lou H, Sun L, Ji M. Synthesis and biological evaluation of curcumin derivatives with water-soluble groups as potential antitumor agents: An in vitro investigation using tumor cell lines. Molecules. 2015 Dec 2;20(12):21501–14.
12. Tao L, Jin L, Dechun L, Hongqiang Y, Changhua K, Guijun L. Galectin-3 expression in colorectal cancer and its correlation with clinical pathological characteristics and prognosis. Open Medicine (Poland). 2017;12(1):226–30.
13. Irving MH, Catchpole B. Anatomy and physiology of the colon, rectum, and anus. British Medical Journal. 1992;304(6834):1106–8.
14. Holdstock DJ, Misiewicz JJ, Smith T, Rowlands EN. Propulsion (mass movements) in the human colon and its relationship to meals and somatic activity. Gut. 1970;11(2):91–9.
15. Encyclopedia Britannica. Large intestine. 12 March. 2020.
16. Ilhan ZE, Marcus AK, Kang D, Rittmann BE. pH-Mediated Microbial and Metabolic. mSphere. 2017;2(3):1–12.
17. Centre M, Evans DF, Pye G, Bramley R, Clark a G, Dyson TJ, et al. Measurement of gastrointestinal pH profiles in normal ambulant human subjects. Gut. 1988;29(8):1035-1041 ST-Measurement of gastrointestinal pH.
18. Stintzing S. Management of colorectal cancer. F1000Prime Reports.

2014;6(November).

19. Mármol I, Sánchez-de-Diego C, Dieste AP, Cerrada E, Yoldi MJR. Colorectal carcinoma: A general overview and future perspectives in colorectal cancer. International Journal of Molecular Sciences. 2017;18(1).
20. Fan X, Zhu M, Qiu F, Li W, Wang M, Guo Y, et al. Curcumin may be a potential adjuvant treatment drug for colon cancer by targeting CD44. International Immunopharmacology. 2020;88(December 2019):106991.
21. Štabuc B. Systemic therapy for colorectal cancer. Archive of Oncology. 2003;11(4):255–63.
22. Patil R, Bellary S. Machine learning approach in melanoma cancer stage detection. Journal of King Saud University - Computer and Information Sciences. 2020;(xxxx).
23. MayoClinic. Colon cancer stages.
24. Gu MJ, Huang QC, Bao CZ, Li YJ, Li XQ, Ye D, et al. Attributable causes of colorectal cancer in china. BMC Cancer. 2018;18(1):1–9.
25. Arroll B. The diagnostic value of symptoms for colorectal cancer in primary care [1]. British Journal of General Practice. 2011;61(588):440.
26. Bethesda M. Stages of Colon Cancer. National Cancer Institute. 2020.
27. Law S, Lo C, Han J, Yang F, Leung AW, Xu C. Design, Synthesis and Characterization of Novel Curcumin Derivatives. Nat Prod Chem Res. 2020;8:1–17.
28. Khor PY, Mohd Aluwi MFF, Rullah K, Lam KW. Insights on the synthesis of asymmetric curcumin derivatives and their biological activities. European Journal of Medicinal Chemistry. 2019;183:111704.
29. Pandit RS, Gaikwad SC, Agarkar GA, Gade AK, Rai M. Curcumin

nanoparticles: physico-chemical fabrication and its in vitro efficacy against human pathogens. 3 Biotech. 2015;5(6):991–7.

30. Salem M, Rohani S, Gillies ER. Curcumin, a promising anti-cancer therapeutic: A review of its chemical properties, bioactivity and approaches to cancer cell delivery. RSC Advances. 2014;4(21):10815–29.

31. Bong PH. Spectral and photophysical behaviors of curcumin and curcuminoids. Bulletin of the Korean Chemical Society. 2000;21(1):81–6.

32. National G, Pillars H. The molecular targets and therapeutic uses of curcumin in health and disease. 2007. 109–117 p.

33. Jiang D, Rasul A, Batool R, Sarfraz I, Hussain G, Mateen Tahir M, et al. Potential Anticancer Properties and Mechanisms of Action of Formononetin. BioMed Research International. 2019;2019:645–51.

34. Priyadarsini KI. The chemistry of curcumin: From extraction to therapeutic agent. Vol. 19, Molecules. MDPI AG; 2014. p. 20091–112.

35. Ma Z, Wang N, He H, Tang X. Pharmaceutical strategies of improving oral systemic bioavailability of curcumin for clinical application. Vol. 316, Journal of Controlled Release. Elsevier B.V.; 2019. p. 359–80.

36. Karthikeyan A, Senthil N, Min T. Nanocurcumin: A Promising Candidate for Therapeutic Applications. Frontiers in Pharmacology. 2020;11(May):1–24.

37. Mbese Z, Khwaza V, Aderibigbe BA. Curcumin and Its Derivatives as Potential Therapeutic Agents in Prostate, Colon and Breast Cancers. Vol. 24, Molecules (Basel, Switzerland). NLM (Medline); 2019.

38. Das S. Pectin based multi-particulate carriers for colon-specific delivery of therapeutic agents. Vol. 605, International Journal of Pharmaceutics. Elsevier B.V.; 2021.

39. Eliaz I, Raz A. Pleiotropic effects of modified citrus pectin. Vol. 11, Nutrients. MDPI AG; 2019.

40. Ciriminna R, Fidalgo A, Delisi R, Tamburino A, Carnaroglio D, Cravotto G, et al. Controlling the Degree of Esterification of Citrus Pectin for Demanding Applications by Selection of the Source. ACS Omega. 2017 Nov 30;2(11):7991–5.

41. Wang C, Qiu WY, Chen TT, Yan JK. Effects of structural and conformational characteristics of citrus pectin on its functional properties. Food Chemistry. 2021;339(May 2020):128064.

42. Venzon SS, Canteri MHG, Granato D, Demczuk B, Maciel GM, Stafussa AP, et al. Physicochemical properties of modified citrus pectins extracted from orange pomace. Journal of Food Science and Technology. 2015 Jul 1;52(7):4102–12.

43. Cao J, Yang J, Wang Z, Lu M, Yue K. Modified citrus pectins by UV/H2O2 oxidation at acidic and basic conditions: Structures and in vitro anti-inflammatory, anti-proliferative activities. Carbohydrate Polymers. 2020;247(February).

44. Lau ES, Liu E, Paniagua SM, Sarma AA, Zampierollo G, López B, et al. Galectin-3 Inhibition With Modified Citrus Pectin in Hypertension. JACC: Basic to Translational Science. 2021 Jan 1;6(1):12–21.

45. Barrow H, Rhodes JM, Yu LG. The role of galectins in colorectal cancer progression. Vol. 129, International Journal of Cancer. 2011. p. 1–8.

46. Schmidt US, Koch L, Rentschler C, Kurz T, Endreß HU, Schuchmann HP. Effect of Molecular Weight Reduction, Acetylation and Esterification on the Emulsification Properties of Citrus Pectin. Food Biophysics. 2015 Jun

18;10(2):217–27.

47. Cisterna BA, Kamaly N, Choi W Il, Tavakkoli A, Farokhzad OC, Vilos C. Targeted nanoparticles for colorectal cancer. Nanomedicine. 2016;11(18):2443–56.

48. Wai WW, AlKarkhi AFM, Easa AM. Comparing biosorbent ability of modified citrus and durian rind pectin. Carbohydrate Polymers. 2010 Feb 11;79(3):584–9.

49. Zhang W, Xu P, Zhang H. Pectin in cancer therapy: A review. Trends in Food Science and Technology. 2015;44(2):258–71.

50. Fracasso AF, Perussello CA, Carpiné D, Petkowicz CL de O, Haminiuk CWI. Chemical modification of citrus pectin: Structural, physical and rheologial implications. International Journal of Biological Macromolecules. 2018;109:784–92.

51. Kolatsi-Joannou M, Price KL, Winyard PJ, Long DA. Modified citrus pectin reduces galectin-3 expression and disease severity in experimental acute kidney injury. PLoS ONE. 2011;6(4).

52. Bailly C. Potential use of edaravone to reduce specific side effects of chemo-, radio- and immuno-therapy of cancers. International Immunopharmacology. 2019;77(September):105967.

53. Sabra R, Billa N, Roberts CJ. An augmented delivery of the anticancer agent, curcumin, to the colon. Reactive and Functional Polymers [Internet]. 2018;123(December 2017):54–60. Available from: https://doi.org/10.1016/j.reactfunctpolym.2017.12.012

54. Hait WN. Anticancer drug development: The grand challenges. Vol. 9, Nature Reviews Drug Discovery. 2010. p. 253–4.

55. Cao J, Yang J, Wang Z, Lu M, Yue K. Modified citrus pectins by UV/H2O2 oxidation at acidic and basic conditions: Structures and in vitro anti-inflammatory, anti-proliferative activities. Carbohydrate Polymers. 2020;247(July).

56. Glinsky V V., Raz A. Modified citrus pectin anti-metastatic properties: one bullet, multiple targets. Carbohydrate Research. 2009;344(14):1788–91.

57. Jacob EM, Borah A, Jindal A, Pillai SC, Yamamoto Y, Maekawa T, et al. Synthesis and characterization of citrus-derived pectin nanoparticles based on their degree of esterification. Journal of Materials Research. 2020 Jun 29;35(12):1514–22.

58. Wang W, Feng Y, Chen W, Adie K, Liu D, Yin Y. Citrus pectin modified by microfluidization and ultrasonication: Improved emulsifying and encapsulation properties. Ultrasonics Sonochemistry. 2021;70(September 2020):105322.

59. Hu Q, Luo Y. Chitosan-based nanocarriers for encapsulation and delivery of curcumin: A review. International Journal of Biological Macromolecules. 2021;179:125–35.

60. Fan W, Yan W, Xu Z, Ni H. Formation mechanism of monodisperse, low molecular weight chitosan nanoparticles by ionic gelation technique. Colloids and Surfaces B: Biointerfaces. 2012;90(1):21–7.

61. Samrot A V., Burman U, Philip SA, Shobana N, Chandrasekaran K. Synthesis of curcumin loaded polymeric nanoparticles from crab shell derived chitosan for drug delivery. Informatics in Medicine Unlocked. 2018;10(December 2017):159–82.

62. Jhaveri J, Raichura Z, Khan T, Momin M, Omri A. Chitosan nanoparticles-insight into properties, functionalization and applications in drug delivery and

theranostics. Molecules. 2021;26(2).

63. Afzali E, Eslaminejad T, Yazdi Rouholamini SE, Shahrokhi-Farjah M, Ansari M. Cytotoxicity effects of curcumin loaded on chitosan alginate nanospheres on the KMBC-10 spheroids cell line. International Journal of Nanomedicine. 2021;16:579–89.

64. Khan I, Saeed K, Khan I. Nanoparticles: Properties, applications and toxicities. Arabian Journal of Chemistry. 2019;12(7):908–31.

65. Soares S, Sousa J, Pais A, Vitorino C. Nanomedicine : Principles , Properties , and Regulatory Issues. 2018;6(August):1–15.

66. Khodabandehloo H, Zahednasab H, Hafez AA. Nanocarriers usage for drug delivery in cancer therapy. International Journal of Cancer Management. 2016;9(2).

67. Hua S, Wu SY. Editorial: Advances and challenges in nanomedicine. Vol. 9, Frontiers in Pharmacology. Frontiers Media S.A.; 2018.

68. Hua S, de Matos MBC, Metselaar JM, Storm G. Current trends and challenges in the clinical translation of nanoparticulate nanomedicines: Pathways for translational development and commercialization. Vol. 9, Frontiers in Pharmacology. Frontiers Media S.A.; 2018.

69. Wu LP, Wang D, Li Z. Grand challenges in nanomedicine. Vol. 106, Materials Science and Engineering C. Elsevier Ltd; 2020.

70. Metselaar JM, Lammers T. Challenges in nanomedicine clinical translation. Drug Delivery and Translational Research. 2020 Jun 1;10(3):721–5.

71. Sabra R, Billa N, Roberts CJ. An augmented delivery of the anticancer agent, curcumin, to the colon. Reactive and Functional Polymers. 2018;123(December 2017):54–60.

72. Giri TK. 5 - Nanoarchitectured Polysaccharide-Based Drug Carrier for Ocular Therapeutics. In: Holban AM, Grumezescu AM, editors. Nanoarchitectonics for Smart Delivery and Drug Targeting. William Andrew Publishing; 2016. p. 119–41.

73. Sabra R, Roberts CJ, Billa N. Courier properties of modified citrus pectinate-chitosan nanoparticles in colon delivery of curcumin. Colloid and Interface Science Communications. 2019;32(August):100192.

74. Aslantürk ÖS. In Vitro Cytotoxicity and Cell Viability Assays: Principles, Advantages, and Disadvantages. In: Genotoxicity - A Predictable Risk to Our Actual World. InTech; 2018.

75. Leclere L, Fransolet M, Cote F, Cambier P, Arnould T, Van Cutsem P, et al. Heat-modified citrus pectin induces apoptosis-like cell death and autophagy in HepG2 and A549 cancer cells. PLoS ONE. 2015;10(3):1–24.

76. Fracasso AF, Perussello CA, Carpiné D, Petkowicz CL de O, Haminiuk CWI. Chemical modification of citrus pectin: Structural, physical and rheologial implications. International Journal of Biological Macromolecules. 2018 Apr 1;109:784–92.

77. Chuah LH, Billa N, Roberts CJ, Burley JC, Manickam S. Curcumin-containing chitosan nanoparticles as a potential mucoadhesive delivery system to the colon. Pharmaceutical development and technology. 2013;18(3):591–9.

78. Prohens R, Puigjaner Vallet MaC. Crystal engineering studies: polymorphs and co-crystals. Handbook of Instrumental Techniques from CCiTUB. 2012;(January):45–124.

79. Nair RS, Morris A, Billa N, Leong CO. An Evaluation of Curcumin-Encapsulated Chitosan Nanoparticles for Transdermal Delivery. AAPS

PharmSciTech. 2019;20(2):1–13.

80. Morris GA, Foster TJ, Harding SE. The effect of the degree of esterification on the hydrodynamic properties of citrus pectin. Food Hydrocolloids. 2000;14(3):227–35.

81. Valencia MS, Silva Júnior MF da, Xavier-Júnior FH, Veras B de O, Albuquerque PBS de, Borba EF de O, et al. Characterization of curcumin-loaded lecithin-chitosan bioactive nanoparticles. Carbohydrate Polymer Technologies and Applications. 2021;2:100119.

82. Levi S, Rac V, Manojlovi V, Raki V, Bugarski B, Flock T, et al. Limonene encapsulation in alginate/poly (vinyl alcohol). Procedia Food Science. 2011;1:1816–20.

83. Shen S, Wu Y, Liu Y, Wu D. High drug-loading nanomedicines: Progress, current status, and prospects. Vol. 12, International Journal of Nanomedicine. Dove Medical Press Ltd.; 2017. p. 4085–109.

84. Shin GH, Chung SK, Kim JT, Joung HJ, Park HJ. Preparation of chitosan-coated nanoliposomes for improving the mucoadhesive property of curcumin using the ethanol injection method. Journal of Agricultural and Food Chemistry. 2013 Nov 20;61(46):11119–26.

85. Venzon SS, Canteri MHG, Granato D, Demczuk B, Maciel GM, Stafussa AP, et al. Physicochemical properties of modified citrus pectins extracted from orange pomace. Journal of Food Science and Technology. 2015;52(7):4102–12.

86. Shin GH, Chung SK, Kim JT, Joung HJ, Park HJ. Preparation of chitosan-coated nanoliposomes for improving the mucoadhesive property of curcumin using the ethanol injection method. Journal of Agricultural and Food

Chemistry. 2013 Nov 20;61(46):11119–26.

87. Hwang SW, Shin JS. Pectin-coated curcumin-chitosan microparticles crosslinked with Mg2+ for delayed drug release in the digestive system. International Journal of Polymer Science. 2018;2018.

88. Maciel VBV, Yoshida CMP, Pereira SMSS, Goycoolea FM, Franco TT. Electrostatic self-assembled chitosan-pectin nano- and microparticles for insulin delivery. Molecules. 2017 Oct 1;22(10).

89. Thanh NTK, Maclean N, Mahiddine S. Mechanisms of nucleation and growth of nanoparticles in solution. Vol. 114, Chemical Reviews. American Chemical Society; 2014. p. 7610–30.

90. Panyam J, Dali MM, Sahoo SK, Ma W, Chakravarthi SS, Amidon GL, et al. Polymer degradation and in vitro release of a model protein from poly(D,L-lactide-co-glycolide) nano- and microparticles. Journal of Controlled Release. 2003 Sep 19;92(1–2):173–87.

91. Singh R, Lillard JW. Nanoparticle-based targeted drug delivery. Vol. 86, Experimental and Molecular Pathology. 2009. p. 215–23.

92. Chuah LH, Billa N, Roberts CJ, Burley JC, Manickam S. Curcumin-containing chitosan nanoparticles as a potential mucoadhesive delivery system to the colon. Pharmaceutical development and technology. 2013;18(3):591–9.

93. Sabra R, Roberts CJ, Billa N. Courier properties of modified citrus pectinate-chitosan nanoparticles in colon delivery of curcumin. Colloid and Interface Science Communications. 2019 Sep;32:100192.

94. Cardoso ACF, Andrade LN de S, Bustos SO, Chammas R. Galectin-3 determines tumor cell adaptive strategies in stressed tumor microenvironments. Vol. 6, Frontiers in Oncology. Frontiers Media S.A.; 2016.

95. Díaz-Alvarez L, Ortega E. The Many Roles of Galectin-3, a Multifaceted Molecule, in Innate Immune Responses against Pathogens. Vol. 2017, Mediators of Inflammation. Hindawi Limited; 2017.

96. Dong R, Zhang M, Hu Q, Zheng S, Soh A, Zheng Y, et al. Galectin-3 as a novel biomarker for disease diagnosis and a target for therapy (Review). Vol. 41, International Journal of Molecular Medicine. Spandidos Publications; 2018. p. 599–614.

97. Rocha D. Natural products in anticancer therapy.

98. Reddy L, Odhav B, Bhoola KD. Natural products for cancer prevention: A global perspective. Vol. 99, Pharmacology and Therapeutics. Elsevier Inc.; 2003. p. 1–13.

99. Sparreboom A, Scripture CD, Trieu V, Williams PJ, De T, Yang A, et al. Comparative Preclinical and Clinical Pharmacokinetics of a Cremophor-Free, Nanoparticle Albumin-Bound Paclitaxel (ABI-007) and Paclitaxel Formulated in Cremophor (Taxol) [Internet]. Available from: www.aacrjournals.org

APPENDIX

Appendix A: Table 3.1: Effect of varying STPP concentration on size and zeta potential of MCP-NPs.

MCP formulation	STPP concentration (mg/mL)	Size (nm)	Zeta-charge (mV)
STPP-MCP1-NPS	0.5	240.6 ± 0.60	5.83 ± 0.01
	0.7	283.3 ± 4.50	4.09 ± 0.01
	1.0	342.0 ± 2.00	3.31 ± 0.42
STPP-MCP2-NPS	0.5	354.5 ± 1.50	2.70 ± 0.01
	0.7	361.7 ± 0.67	1.18 ± 0.05
	1.0	367.8 ± 0.76	1.86 ± 0.01
STPP-MCP4-NPS	0.5	463.3 ± 0.78	1.21 ± 0.01
	0.7	453.9 ± 1.11	-3.64 ± 0.01
	1.0	533.7 ± 0.50	-4.52 ± 0.02

Appendix B: Table 3.2: Effect of varying CS concentrations on size and zeta potential of MCP-NPs formulations.

MCP formulation	CS concentration (mg/mL)	Size (nm)	Zeta-potential (mV)
CS-MCP1-NPS	0.5	173.6 ± 0.35	4.56 ± 0.01
	0.7	227.4 ± 0.42	4.12 ± 0.02
	1.0	230.0 ± 0.70	3.68 ± 0.01
CS-MCP2-NPS	0.5	235.0 ± 0.70	-3.07 ± 0.04
	0.7	260.5 ± 0.31	-7.65 ± 0.02
	1.0	280.7 ± 0.31	-5.10 ± 0.01
CS-MCP4-NPS	0.5	313.5 ± 1.66	1.04 ± 0.02
	0.7	338.6 ± 0.95	-2.75 ± 0.02
	1.0	365.4 ± 0.60	-6.35 ± 0.02

Appendix C: Table 3.3: Effect of varying STPP amounts on size and zeta potential of CCM-NPs.

Formulation	STPP amount (μL)	Size (nm)	Zeta-potential (mV)
1AC	300	209.4 ± 0.30	10.6 ± 0.02
1BC	400	225.2 ± 0.30	9.42 ± 0.02
1CC	500	257.5 ± 0.62	5.22 ± 0.01

Appendix D: Table 3.4: Effect of varying CS amounts on size and zeta potential of CCM-NPs.

Formulation	CS amount (μL)	Size (nm)	Zeta-potential (mV)
2AC	600	139.3 ± 0.57	16.6 ± 0.07
2BC	700	143.9 ± 0.20	13.7 ± 0.06
2CC	800	159.7 ± 0.46	13.3 ± 0.10

Appendix E: Table 3.5: Effect of varying CUR amounts on size and zeta potential of CCM-NPs.

Formulation	CUR amount (μL)	Size (nm)	Zeta-potential (mV)
3AC	100	651.3 ± 0.40	6.44 ± 0.006
3BC	200	545.3 ± 0.10	7.51 ± 0.006
3CC	300	351.1 ± 0.53	9.74 ± 0.03
3DC	400	412.9 ± 0.31	8.93 ± 0.06